Physical Cosmology
Sommersemester 2009
Lecture Notes

Jochen Weller
Universitätssternwarte
Ludwigs-Maximilians-Universität München

April 14, 2009

Contents

Chapter 1

Introduction

$\hbar = c = k = 1$.

1.1 Timetable

Lecture:
Fridays: 14:30-16:00
Problem classes:
Fridays (dates to be announced): 12:00-13:30

1.2 Bibliography

Ray d'Inverno, *Introducing Einstein's Relativity*, Oxford University Press.
Sean M. Carroll, *Spacetime and Geometry*, Addison Wesley.
Steven Weinberg, *Gravitation and Cosmology*, Wiley & Sons.
Malcolm S. Longair, *Galaxy Formation*, Springer.
Marc L. Kutner, *Astronomy: A Physical Perspective*, Cambridge University Press.

Chapter 2

Cosmography

2.1 Relativistic Cosmology

2.1.1 The Cosmological Principle

As a generalization of the Copernican principle that the Earth is not at the centre of the solar system, the *cosmological principle* states that we do not occupy a special point in the universe, actually that there is *no* special point in the universe.

> **The cosmological principle:** At each epoch, the universe presents the same aspect from every point, except for local irregularities.

Mathematically this means that there exists a cosmic time t and that each constant time slice is homogeneous *and* isotropic. Globally isotropic manifolds are homogeneous, so the cosmological principle requires that space-time can be foliated into space-like hypersurfaces which are spherically symmetric about each point. Homogeneity has to be understood like homogeneity of gas, which is not homogeneous microscopically but on large scales.

2.1.2 Weyl's Postulate

Hermann Weyl assumed 1923 that there is a privileged class of observers associated with the smeared-out motion of galaxies. This follows the fact that the relative motion in groups of galaxies is small.

Weyl's postulate: The particles of the substratum lie in space-time on a congruence of time-like geodesics diverging from a point in the finite or infinite past.

Weyl introduced the 'substratum' or fluid pervading space in which galaxies move like fundamental particles in a fluid, which follow a special motion. The postulate requires that the geodesics of these particles do not intercept. There is a *unique* geodesic in each point of space-time and hence each 'matter' particle possesses a unique velocity. Hence the substratum may be taken as a *perfect fluid*. Note that the motions of galaxies deviate from this, but this deviation is random and it's velocity is less than a thousands of the speed of light, while the general relative motion is of the order of the speed of light.

2.1.3 The Robertson-Walker Metric

Analyse universe which obey the cosmological principle and Weyl's postulate. Hence the geodesics of the fluid particles (substratum) have to be orthogonal to space-like hypersurfaces. We introduce coordinate system (t, x^1, x^2, x^3), where space-like hypersurfaces are given by $t = const.$ and (x^1, x^2, x^3) are constant along geodesic as shown in Fig. 2.1. These coordinates are called *co-moving*. From orthogonality we obtain for the line element (metric)

$$ds^2 = dt^2 - h_{ab}dx^a dx^b \ ,$$

where Latin indices run over the spatial indices $a = 1, 2, 3$. And

$$h_{ab} = h_{ab}(t, \mathbf{x}) \ ,$$

with t corresponding to the cosmic time. If we consider a small triangle given by three particles of the fluid at a given time t and then at a later time, the cosmological principle requires that the second triangle must be geometrically similar to the first and the magnification factor must be independent of the position of the triangle. Therefore time can only enter via a common factor into h_{ab} and hence

$$h_{ab} = [a(t)]^2 g_{ab}(x^a) \ . \tag{2.1}$$

The ratio of two values of $a(t)$ at two different times is the magnification ratio.

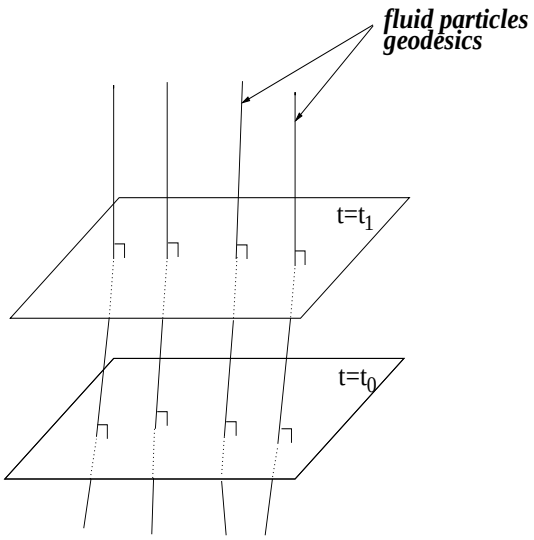

Figure 2.1: Constant cosmic time hypersurfaces and fluid particle geodesics.

In order that the space is homogeneous and isotropic the curvature must be constant, otherwise points are *not* geometrically equal. A space with constant curvature is characterised by

$$R_{\alpha\beta\gamma\delta} = K\left(g_{\alpha\gamma}g_{\beta\delta} - g_{\alpha\beta}g_{\beta\gamma}\right) \ ,$$

with K a constant, called the *curvature*. This must hold for the 3-dimensional metric g_{ab} in Eqn. 2.1. This will lead to the *Ricci tensor*

$$\begin{aligned} R_{bd} &= g^{ac}R_{abcd} \\ &= Kg^{ac}\left(g_{ac}g_{bd} - g_{ad}g_{bc}\right) \\ &= K\left(3g_{bd} - g_{bd}\right) \\ &= 2Kg_{bd} \end{aligned} \tag{2.2}$$

and hence the Ricci or curvature scalar of $R = g^{bd}R_{bd} = 6K$ is constant. Because the 3-space has to be isotropic about every point it must be spherical symmetric about every point. This has the general spatial metric (show with d'Inverno 14.33 as an Exercise !)

$$d\sigma^2 = e^{\lambda}dr^2 + r^2\left(d\theta^2 + \sin^2\theta d\phi^2\right) \ ,$$

with $\lambda = \lambda(r)$. And the non-vanishing components Exercise ! of the Ricci tensor are

$$R_{11} = \lambda'/r\,, \qquad R_{22} = R_{33}/\sin^2\theta = 1 + \frac{1}{2}re^{-\lambda}\lambda' - e^{-\lambda}\,,$$

and hence the condition of constant curvature Eqn. 2.2 leads to

$$\lambda'/r = 2Ke^{\lambda}\,, \qquad 1 + \frac{1}{2}re^{-\lambda}\lambda' - e^{-\lambda} = 2Kr^2\,,$$

with the solution

$$e^{-\lambda} = 1 - Kr^2\,.$$

Therefore an isotropic 3-space of constant curvature has the metric

$$d\sigma^2 = \frac{dr^2}{1-Kr^2} + r^2\left(d\theta^2 + \sin^2\theta\, d\phi^2\right)\,. \tag{2.3}$$

For the space-time metric we absorb the arbitrariness of the magnitude of K into the scale factor $a(t)$ by defining $K = k|K|$ and the rescaled radial coordinate

$$r^* = |K|^{1/2}r\,,$$

and we obtain

$$ds^2 = dt^2 - \frac{[a(t)]^2}{|K|}\left[\frac{dr^{*2}}{1-kr^{*2}} + r^{*2}\left(d\theta^2 + \sin^2\theta d\phi^2\right)\right]$$

and define the rescaled scale function $R(t)$ by

$$\begin{aligned} R(t) &= a(t)/|K|^{1/2} && \text{if } K \neq 0 \\ R(t) &= a(t) && \text{if } K = 0 \end{aligned}$$

and we obtain

$$ds^2 = dt^2 - [R(t)]^2\left[\frac{dr^2}{1-kr^2} + r^2\left(d\theta^2 + \sin^2\theta d\phi^2\right)\right]\,. \tag{2.4}$$

As a warning we have to point out that in this rescaled units, the scale factor has now a length dimension and the coordinates are dimensionless. This is all right as long as we study cosmological models from a theoretical point of view. But as soon as we will discuss more physical quantities we will prefer the form in Eqn. 2.3. Furthermore we can introduce a new radial parameter

$$r = \bar{r}/\left(1 + \frac{1}{4}K\bar{r}^2\right)\,,$$

and drop the bars we get the metric in its conformally flat form Exercise !

$$ds^2 = dt^2 - [R(t)]^2 \frac{dr^2 + r^2\left(d\theta^2 + \sin^2\theta d\phi^2\right)}{\left[1 + \frac{1}{4}kr^2\right]^2}, \qquad (2.5)$$

which is the *Robertson-Walker metric* with $k = +1,-1$ or 0. For $k = +1$ the spatial part is a 3-sphere (S^3) (closed, bounded or compact) and the whole space-time has a cylindrical topology of $\mathbb{R} \times S^3$, with $\mathbb{R}$ for the time coordinate. For $k = 0$ is Euclidean four-dimensional space time $\mathbb{R}^4$ which is called open. For $k = -1$ the spatial part is a 3-dimensional hyperboloid in four-dimensional Minkowski space. The topology is again $\mathbb{R}^4$ and open. Note that we only discussed the simplest topologies possible.

2.1.4 Friedmann Equations

In order to write down the equations which govern the large scale behaviour of the universe we need to solve Einstein's equation for general relativity

$$G_{\alpha\beta} - \Lambda g_{\alpha\beta} = 8\pi G T_{\alpha\beta}\,, \qquad (2.6)$$

where G is Newton's constant of gravity, $G_{\alpha\beta}$ is the Einstein tensor

$$G_{\alpha\beta} = R_{\alpha\beta} - \frac{1}{2} g_{\alpha\beta} R\,,$$

Λ the cosmological constant and $T_{\alpha\beta}$ the energy momentum tensor of the different components in the universe. Note that Greek indices run over $\alpha = 0, 1, 2, 3$. Weyl's postulate requires the 'substratum' to be a perfect fluid. A perfect fluid is characterised by a 4-velocity $u^\alpha = dx^\alpha/d\tau$, where τ is the proper time along the world line, a proper density field $\rho_0(x)$ and a scalar pressure field $p(x)$. The energy - momentum tensor for a pressureless fluid is $T^{\alpha\beta} = \rho_0 u^\alpha u^\beta$ and hence we choose as an ansatz

$$T^{\alpha\beta} = \rho_0 u^\alpha u^\beta + p S^{\alpha\beta}\,,$$

with $S^{\alpha\beta}$ a symmetric tensor due to covariance of the Einstein equations. The only second-rank tensors associated with the fluid are $u^\alpha u^\beta$ and $g^{\alpha\beta}$ and we write

$$S^{\alpha\beta} = \lambda u^\alpha u^\beta + \mu g^{\alpha\beta}\,,$$

with constants λ and μ. The energy-momentum conservation $\partial_\beta T^{\alpha\beta} = 0$ should reproduce the Eulerian equations of Newtonian motion of a perfect

fluid in Minkowski space. If $\lambda = 1$ and $\mu = -1$ Exercise ! we obtain the continuity equation

$$\frac{\partial \rho}{\partial t} + \nabla (\rho \mathbf{u}) = 0$$

and the Navier-Stokes equation

$$\rho \left[\frac{\partial \mathbf{u}}{\partial t} + (\mathbf{u} \cdot \nabla)\mathbf{u} \right] = -\nabla p \,,$$

if there are *no* external forces and the fluid is moving with velocity $\mathbf{u}$ with respect to the observer. Finally we obtain

$$T_{\alpha\beta} = (\rho + p) u_\alpha u_\beta - p g_{\alpha\beta} \,. \qquad (2.7)$$

The preferred coordinate system (Weyl's postulate) is $u^\alpha \equiv (1, 0, 0, 0)$ and we obtain with the the Robertson-Walker metric from Eqn. 2.3 and the Einstein equations in Eqn. 2.6 we obtain for the $\alpha\beta = 00$ component Exercise !

$$-3\frac{\ddot{a}}{a} = 4\pi G(\rho + 3p) - \Lambda \qquad (2.8)$$

and for the $\alpha\beta = ab$ component Exercise !

$$\frac{\ddot{a}}{a} + 2\left(\frac{\dot{a}}{a}\right)^2 + 2\frac{K}{a^2} = 4\pi G(\rho - p) + \Lambda \,, \qquad (2.9)$$

which is only *one* equation because of isotropy. Note that we used the Robertson - Walker metric in its form with the dimensionless scale factor and coordinates of length dimension

$$ds^2 = dt^2 - [a(t)]^2 \left[\frac{dr^2}{1 - Kr^2} + r^2 \left(d\theta^2 + \sin^2\theta \, d\phi^2 \right) \right] . \qquad (2.10)$$

With some simple algebra we obtain the two *Friedmann equations*

$$\frac{\dot{a}^2}{a^2} + \frac{K}{a^2} = \frac{8\pi G}{3}\rho + \frac{\Lambda}{3} \,, \qquad (2.11)$$

$$\frac{\ddot{a}}{a} = -\frac{4\pi G}{3}(\rho + 3p) + \frac{\Lambda}{3} \,. \qquad (2.12)$$

We can combine the two Friedmann equations to obtain

$$\dot{\rho} = -3(\rho + p)\frac{\dot{a}}{a}\,, \tag{2.13}$$

which if we multiply this by a^3 and note that the volume $V \propto a^3$ is the equation for the conservation of energy with

$$dE + pdV = 0\,,$$

where we recognise that the pressure does work in the expansion.

2.1.5 Cosmological Models

We will first introduce some simplifying notations, where their meaning will become clear during the course of this section. First we introduce the Hubble parameter

$$\boxed{H(t) \equiv \frac{\dot{a}}{a}\,,} \tag{2.14}$$

which is the (normalized) expansion rate of the universe. Furthermore we can formally associate an energy density with the cosmological constant

$$\boxed{\rho_\Lambda \equiv \frac{\Lambda}{8\pi G}\,.} \tag{2.15}$$

In this notation the 1st Friedmann equation reads like

$$H^2 + \frac{K}{a^2} = \frac{8\pi G}{3}\left(\sum_i \rho_i + \rho_\Lambda\right)\,, \tag{2.16}$$

where the index i is a label for the kind of particle fluid we study, like matter or radiation. Note that in general we have to sum over all the 'particle' species or energy components in the universe in order to obtain the total energy-momentum tensor. In order to obtain a flat universe we require $K = 0$ and hence

$$\rho_{\rm tot} \equiv \sum_i \rho_i + \rho_\Lambda = \frac{3H^2}{8\pi G} \equiv \rho_{\rm crit}\,.$$

We can define then

$$\boxed{\Omega_i \equiv \frac{\rho_i}{\rho_{\rm crit}}\,, \qquad (2.17)}$$

which is the energy density in units of the critical density $\rho_{\rm crit}$. In this way we can define quantities like Ω_Λ, $\Omega_{\rm m}$ (for matter) and $\Omega_{\rm r}$ for radiation. Note that we define these quantities time dependent and not only at $t_{\rm today}$, if we want to specify the values today we will add an index 0, ie. $\Omega_{i,0}$[1]. With this notation the 1st Friedmann equation becomes

$$\frac{K}{a^2H^2} = \sum_i \Omega_i + \Omega_\Lambda - 1$$

and if we define $\Omega_k \equiv -K/(aH)^2$

$$\boxed{1 = \sum_i \Omega_i + \Omega_\Lambda + \Omega_k\,. \quad (2.18)}$$

Note that the sign of the definition of Ω_k varies in the literature.

In the following we will only discuss models with pressureless matter with $p = 0$. In general the flat cosmologies we discuss here, which obey the cosmological principle and Weyl's postulate, are called *Friedmann-Robertson-Walker or FRW models*. For pressureless matter we obtain with the energy conservation equation Eqn. 2.13

$$\rho_{\rm m} = \rho_{\rm m,0} \left(\frac{a}{a_0}\right)^{-3}\,,$$

where $\rho_{\rm m,0}$ is the energy density in matter today and a_0 is the scale factor today. Note that we choose

$$\boxed{a_0 \equiv 1 \quad (2.19)}$$

in the rest of the lecture, unless otherwise noted. The 1st Friedmann equation for a flat (K=0) universe can then be written as

$$\left(\frac{\dot a}{a}\right)^2 = \frac{8\pi G}{3}\rho_{\rm m,0}a^{-3} + \frac{\Lambda}{3}\,, \qquad (2.20)$$

[1]Note that in most articles and books $\Omega_{\rm m}$ and Ω_Λ etc. refer actually to the densities today.

or

$$\dot{a}^2 = H_0^2 \Omega_{\mathrm{m},0} a^{-1} + H_0^2 \Omega_{\Lambda,0} a^2 \,, \tag{2.21}$$

with H_0 the Hubble constant (Hubble parameter today). Note that with Eqn. 2.18 we have $\Omega_{\mathrm{m},0} + \Omega_{\Lambda,0} = 1$ in a flat universe.

Let us assume that $\Lambda > 0$ and if we substitute $u = 2\Omega_{\Lambda,0}/\Omega_{\mathrm{m},0} a^3$ we obtain

$$\dot{u}^2 = 9H_0^2 \Omega_{\Lambda,0} \left[2u + u^2\right] = 3\Lambda \left[2u + u^2\right] \,.$$

If we take the positive root of this equation we obtain then

$$\int_0^u \frac{du}{(2u+u^2)^{1/2}} = \int_0^t (3\Lambda)^{1/2}\, dt = (3\Lambda)^{1/2} t \,,$$

where we assume a big bang model with $a = 0$ at $t = 0$. This can be integrated by completing the square in the u-integral and substitutions $v = u + 1$ and $\cosh w = v$

$$\int_0^u \frac{du}{\left[(u+1)^2 - 1\right]^{1/2}} = \int_1^v \frac{dv}{(v^2-1)^{1/2}} = \int_0^w \frac{\sinh w dw}{\left(\cosh^2 w - 1\right)^{1/2}} = \int_0^w dw = w$$

and we obtain finally the time evolution of the scale factor

$$a^3 = \frac{\Omega_{\mathrm{m},0}}{2\Omega_{\Lambda,0}} \left[\cosh(3\Lambda)^{1/2} t - 1\right] \,.$$

If $\Lambda < 0$ we introduce $u = -2\Omega_{\Lambda,0}/\Omega_{\mathrm{m},0} a^3$ and then obtain as above

$$a^3 = \frac{\Omega_{\mathrm{m},0}}{2(-\Omega_{\Lambda,0})} \left\{1 - \cos\left[3(-\Lambda)\right]^{1/2} t\right\} \,.$$

For $\Lambda = 0$ we have

$$\boxed{a = \left(\frac{9}{4} H_0^2 t^2\right)^{1/3} \,, \quad (2.22)}$$

which is called the *Einstein-de Sitter model*. The Hubble parameter for this model is

$$H(t) = \frac{\dot{a}}{a} = \frac{2}{3t} \,.$$

If we have a non-vanishing cosmological constant Λ the flat pressureless

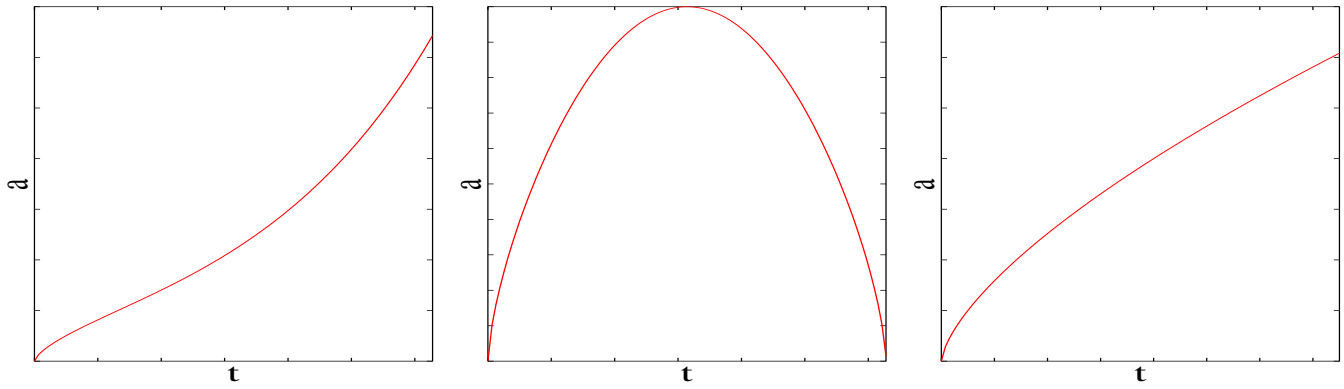

Figure 2.2: The three flat, pressureless cosmological models. On the left $\Lambda > 0$, in the middle $\Lambda < 0$ and on the right the Einstein de-Sitter model with $\Lambda = 0$.

models behave initially like an Einstein-de Sitter model since the first term in Eqn. 2.20 dominates for small scale factors a over the cosmological constant term.

The qualitative behaviour of the flat, pressureless solution can be studied when we look at the right hand side of Eqn. 2.21. For $\Lambda < 0$ $\dot{a}$ vanishes at

$$a = a_m = \left[-\frac{\Omega_{\mathrm{m},0}}{\Omega_{\Lambda,0}} \right]^{1/3} ,$$

which is a local maximum Exercise !. For $\Lambda \geq 0$ the solution grows without bound. For large t and $\Lambda > 0$ the second term in Eqn. 2.20 dominates and we obtain

$$a \propto \exp\left[(\Lambda/3)^{1/2}\, t \right] ,$$

which grows exponentially with time.

We will now discuss non-flat models ($K \neq 0$) but with a vanishing cosmological constant ($\Lambda = 0$). We then have to solve

$$\dot{a}^2 = \Omega_{\mathrm{m},0} H_0^2 a^{-1} - K = \Omega_{\mathrm{m},0} H_0^2 a^{-1} + \Omega_{\mathrm{k},0} H_0^2 \,. \tag{2.23}$$

Note that for $\Lambda = 0$ we have $\Omega_{\mathrm{k},0} = 1 - \Omega_{\mathrm{m},0}$. For $K > 0$ ($\Omega_{\mathrm{k}} < 0$) we substitute $u^2 = a/(\Omega_{\mathrm{m},0} H_0^2)$ and obtain

$$\dot{u}^2 = \frac{u^{-2} H_0^2 |\Omega_{\mathrm{k},0}|^3}{4\Omega_{\mathrm{m},0}^2} \left[u^{-2} - 1 \right] .$$

When we substitute $u = \sin\theta$ we can integrate this differential equation and obtain

$$t = c_1 \left\{ \sin^{-1}\left[\frac{a}{c_1}\right]^{1/2} - \left[\frac{a}{c_1}\right]^{1/2}\left[1 - \frac{a}{c_1}\right]^{1/2} \right\}, \tag{2.24}$$

with $c_1 = \Omega_{\mathrm{m},0}/(|\Omega_{\mathrm{k},0}|^{3/2}H_0)$. Similarly for $\Lambda = 0$, $K < 0$ ($\Omega_{\mathrm{k}} > 0$) we obtain Exercise !

$$t = c_1 \left\{ -\sinh^{-1}\left[\frac{a}{c_1}\right]^{1/2} + \left[\frac{a}{c_1}\right]^{1/2}\left[1 + \frac{a}{c_1}\right]^{1/2} \right\}.$$

Again we can analyse when the right hand side of Eqn. 2.23 is vanishing and we find that for $K > 0$ we have a local maximum at

$$a_m = \frac{\Omega_{\mathrm{m},0}}{|\Omega_{\mathrm{k},0}|} \tag{2.25}$$

For $K < 0$ we have growth without bounds. For $K < 0$ the curvature term is dominating for large a with $\dot{a}^2 \propto 1$ and $a \propto t$. Note that all other cases

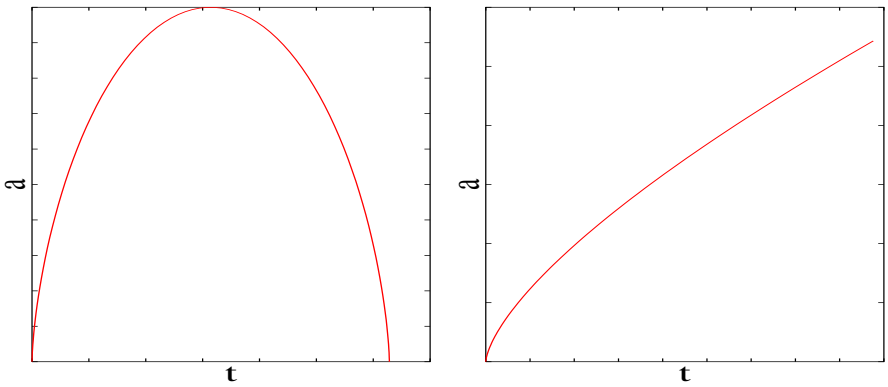

Figure 2.3: The two non-flat FRW models with vanishing cosmological constant $\Lambda = 0$. On the left with $k = +1$ and on the right with $k = -1$.

are slightly more involved and we refer the student to the literature (see d'Inverno chapter 23).

Finally we will discuss the de Sitter model which are flat universes devoid of matter ($\rho = 0$) with a positive cosmological constant. In this case we have

$$a = \exp\left[\left(\frac{1}{3}\Lambda\right)^{1/2} t\right], \tag{2.26}$$

where we chose $a = 1$ at $t = 0$.

2.2 Redshift and Distances

2.2.1 Redshift

In order to study the influence of the expansion of the universe on light emitted by a distant galaxy and received by an observer at the origin we exploit the fact that propagation of light in general relativity is along a null geodesic. If we put the observer at the origin with $r = 0$ and choose a radial null geodesic we get

$$ds^2 = d\theta = d\phi = 0$$

and hence from Eqn. 2.10

$$\frac{dt}{a(t)} = \pm \frac{dr}{(1 - Kr^2)^{1/2}}\,, \tag{2.27}$$

where the + sign corresponds to an emitted light ray and the − sign to a received one. For light ray emitted at time t_1 and a distance r_1 which is received at the origin at time t_0 we obtain

$$\begin{aligned} \int_{t_1}^{t_0} \frac{dt}{a(t)} &= -\int_{r_1}^{0} \frac{dr}{(1-Kr^2)^{1/2}} = \frac{1}{|K|^{1/2}} \int_{0}^{|K|^{1/2} r_1} \frac{dr^*}{(1-kr^{*2})^{1/2}} \\ &= \frac{1}{|K|^{1/2}} S_k^{-1}\left(|K|^{1/2} r_1\right) \quad , \end{aligned} \tag{2.28}$$

with

$$S_k(x) = \begin{cases} \sin(x) & \text{if } K > 0 \quad \text{or} \quad \Omega_{\rm k} < 0\,, \\ x & \text{if } K = 0 \quad \text{or} \quad \Omega_{\rm k} = 0\,, \\ \sinh(x) & \text{if } K < 0 \quad \text{or} \quad \Omega_{\rm k} > 0\,, \end{cases}$$

where we have used for the second equation the substitution $r^* = |K|^{1/2} r$ with $K = k|K|$. Now in order to understand how the frequency ν_0 (wavelength) of the received light behaves in relation to the emitted frequency ν_1. The time when a second wavefront arrives $t_0 + dt_0$ which has been emitted after a short time dt_1 is again given by

$$\int_{t_1+dt_1}^{t_0+dt_0} \frac{dt}{a(t)} = \frac{1}{|K|^{1/2}} S_k^{-1}(|K|^{1/2} r_1)\,,$$

where the right hand side does not change because of Weyl's postulate that the 'substratum' (galaxies) have constant coordinates. So we finally find the

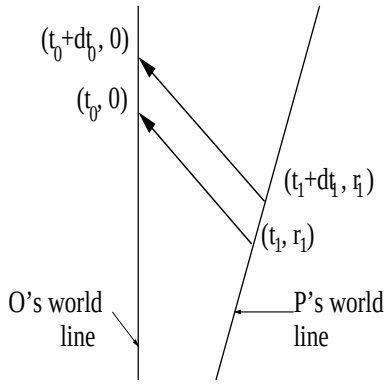

Figure 2.4: Propagation of light rays.

relation between the time difference of the two signals

$$\frac{dt_0}{a\left(t_0\right)} = \frac{dt_1}{a\left(t_1\right)}$$

and hence the relation of the emitted (ν_1) and received (ν_0) frequencies is given by

$$\frac{\nu_0}{\nu_1} = \frac{dt_1}{dt_0} = \frac{a\left(t_1\right)}{a\left(t_0\right)},$$

which is usually expressed by the redshift parameter

$$\boxed{z \equiv \frac{\lambda_0 - \lambda_1}{\lambda_1} = \frac{a\left(t_0\right)}{a\left(t_1\right)} - 1\,, \qquad (2.29)}$$

where λ_1 and λ_0 are the wavelength corresponding to ν_1 and ν_0. Light from a distant object is usually redshifted[2]. Note that if we put the observer at t_0 today and use $a_0 = 1$ we obtain

$$\boxed{a = \frac{1}{1+z} \qquad (2.30)}$$

2.2.2 Proper and Angular Diameter Distance

Because of Weyl's postulate there is a world time and one can define the absolute distance between 'substratum' particles by looking at their position at the *same* world time. If we set $dt = d\theta = d\phi = 0$ in Eqn. 2.10 and assume

[2]Note that in a collapsing universe it is actually blueshifted.

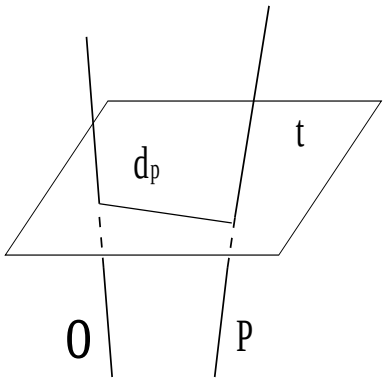

Figure 2.5: Distance between two fluid particles.

one particle is at the origin and the other at r_1 we obtain as the *proper* distance

$$d_p = a(t) \int_0^{r_1} \frac{dr}{(1 - Kr^2)^{1/2}} ,$$

however this requires a *synchronous* measurement of the distance which is of no practical use. One more practical method would be to compare the known absolute luminosity of an object with its observed apparent luminosity or the true diameter with the observed angular diameter.

In this section we consider the second method, while in the next section we will concentrate on the luminosity measurements. We calculate in the following the angular diameter observed at the origin at $t = t_0$ of a light source of of true proper diameter D at $r = r_1$ and $t = t_1$. We choose the

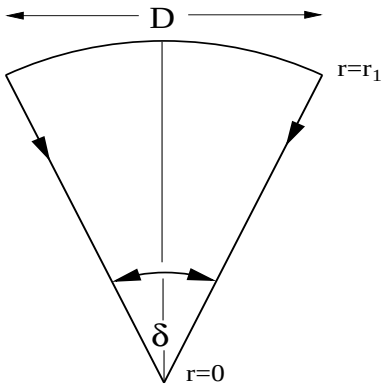

Figure 2.6: Angular diameter distance.

coordinate system like in Fig. 2.6. The light travels then on a cone with a half angle $\theta = \delta/2$. The proper diameter of the source is then given by Eqn. 2.10

$$D = a(t_1) r_1 \delta \qquad \text{for } \delta \ll 1 \,,$$

so we obtain for the angular diameter of the source

$$\delta = \frac{D}{a(t_1) r_1} \,.$$

In Euclidean geometry the angular diameter of a source of diameter D at a distance d is $\delta = D/d$, so we define in *general* the angular diameter distance

$$\boxed{d_{\rm A} \equiv \frac{D}{\delta} \,, \qquad (2.31)}$$

and hence we can write

$$d_{\rm A} = a(t_1) r_1 = \frac{r_1}{1+z} \,.$$

Since we are studying the propagation of light r_1 is given by Eqns. 2.27-2.28 and we obtain

$$\int_{t_1}^{t_0} \frac{dt}{a(t)} = \int_0^z \frac{dz}{H(z)} = \frac{1}{|K|^{1/2}} S_k^{-1}(|K|^{1/2} r_1) \,,$$

where the first equation was obtained by substituting the time integration with a redshift integration and using

$$\frac{dz}{dt} = -\frac{\dot{a}}{a^2} = -\frac{H}{a} \,.$$

and we finally obtain with $|K|^{1/2} = H_0 \sqrt{\Omega_{\rm k,0}}$

$$\boxed{d_A(z) = \frac{1}{\sqrt{|\Omega_k|} H_0 (1+z)} S_k \left(H_0 \sqrt{|\Omega_k|} \int_0^z \frac{dz}{H(z)} \right) \,. \qquad (2.32)}$$

From Eqn. 2.16 we see that the angular diameter distance depends via the Hubble parameter on the cosmological parameters like H_0, $\Omega_{\Lambda,0}$ and $\Omega_{\rm m,0}$. If on could observe the angular diameter distance really accurately one could measure these parameters and also the curvature or general geometry of

the universe. An excellent probe in this way in the anisotropies in cosmic microwave background radiation. One can calculate a typical size of an overdense region at the time the microwave photons start to stream free and we also know the the distance to this last scattering surface. We can compare this with the observed angular size (in form of the anisotropy power spectra) and hence obtain a very accurate measurement of the curvature of the universe.

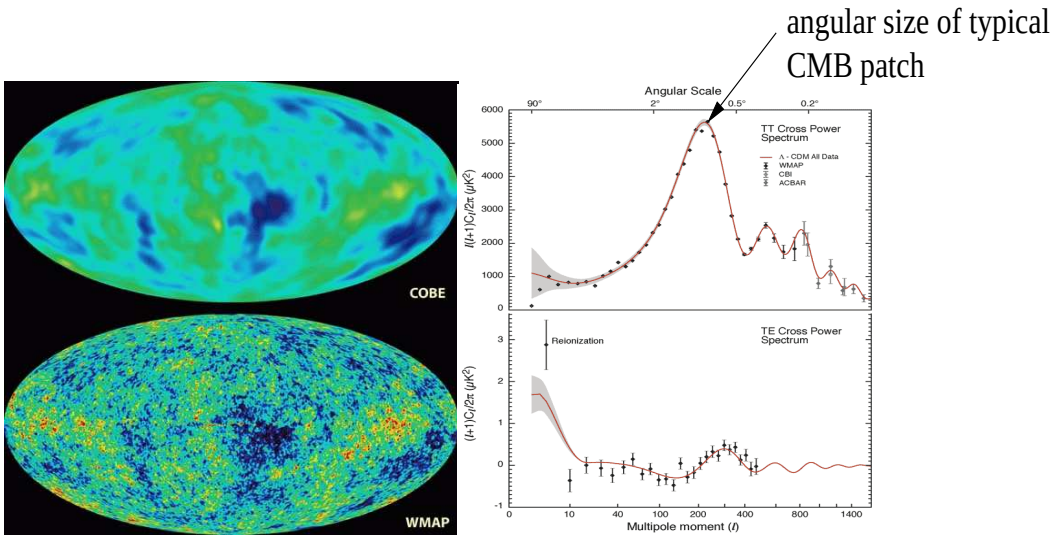

Figure 2.7: Angular anisotropy power spectrum of the cosmic microwave background as observed by the WMAP team (2003).

2.2.3 Luminosity Distance and Deceleration Parameter

As mentioned before another way to measure distance is via comparing the known absolute luminosity of an object with the the observed apparent luminosity. For a telescope mirror with radius b as shown in Fig. 2.8 the solid angle is given by

$$\Delta\Omega = \frac{\pi b^2}{a^2(t_0) r_1^2}$$

and the fraction of isotropically emitted photons that reach telescope is given by ratio of solid angle $\Delta\Omega$ to total solid angle 4π

$$\frac{\Delta\Omega}{4\pi} = \frac{\pi b^2}{4\pi a^2(t_0) r_1^2}$$

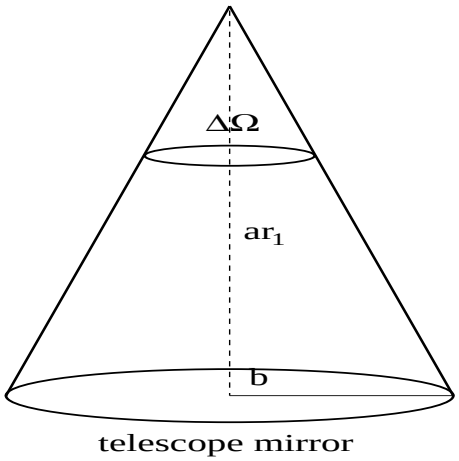

Figure 2.8: The luminosity distance.

If the source has an absolute (or bolometric[3]) luminosity $\mathcal{L}$, which is the total power emitted by the source (in a specified band), the question is what is the received power ? Let us look at a single photon. Photons which are emitted with energy $h\nu_1$ are redshifted to $h\nu_1 a(t_1)/a(t_0) = h\nu_0$. Furthermore photons emitted at intervals δt_1 are received at intervals $\delta t_0 = \delta t_1 a(t_0)/a(t_1)$. So for a single photon we get

$$\begin{aligned} \text{emitted power :} \quad P_{\rm em} &= \tfrac{h\nu_1}{\delta t_1} \\ \text{received power :} \quad P_{\rm rec} &= \tfrac{h\nu_0}{\delta t_0} \\ &= \tfrac{h\nu_1}{\delta t_1}\tfrac{a^2(t_1)}{a^2(t_0)} \ , \end{aligned}$$

hence for the total received power P, we get

$$P = \mathcal{L}\left(\frac{a^2(t_1)}{a^2(t_0)}\right)\frac{A}{4\pi a^2(t_0) r_1^2} \, ,$$

[3]The term bolometric is usually applied when the luminosity is calculated over an entire bandwidth $\Delta\nu$.

where we have used $A = \pi b^2$ for the total mirror area. Now the total apparent luminosity or bolometric flux density is given by

$$\mathcal{F} \equiv \frac{P}{A} = \frac{\mathcal{L} a^2(t_1)}{4\pi r_1^2}\,, \tag{2.33}$$

where we applied $a(t_0) = 1$. In Euclidean space the flux density is given by $\mathcal{F} = \mathcal{L}/(4\pi d^2)$ and this is now generalized to define the *luminosity distance*

$$\boxed{\mathcal{F} = \frac{\mathcal{L}}{4\pi d_{\rm L}^2}\,.} \tag{2.34}$$

Therefore we obtain

$$d_{\rm L} = \frac{r_1}{a} = (1+z) r_1 = (1+z)^2 d_{\rm A}\,,$$

so we finally obtain

$$\boxed{d_{\rm L}(z) = \frac{1+z}{\sqrt{|\Omega_k|}H_0} S_k\left(H_0\sqrt{|\Omega_k|}\int_0^z \frac{dz}{H(z)}\right)\,.} \tag{2.35}$$

It is interesting to note that for low redshifts $z \ll 1$ and small r_1 we have

$$d_A \simeq d_{\rm L} \simeq d_P \simeq r_1$$

and the distinction becomes important only for objects billions of light years away. Therefore we draw our attention to the redshift dependence of the scale factor at late times (or small redshifts). We can Taylor expand the scale factor around $t = t_0$ and obtain

$$a(t) = a(t_0)\left[1 + H_0\,(t - t_0) - \frac{1}{2} q_0 H_0^2 (t_0 - t)^2 + \cdots\right]\,, \tag{2.36}$$

where we used the definition of the Hubble constant $H_0 = \dot{a}(t_0)/a(t_0)$ and we defined the *deceleration parameter*

$$\boxed{q_0 = -\frac{\ddot{a}(t_0)}{a(t_0) H_0^2}\,.} \tag{2.37}$$

As the name already suggests the deceleration parameter quantifies if the expansion of the universe is accelerating ($q_0 < 0$) or decelerating ($q_0 > 0$). It is quite convenient to express the cosmological models from Section 2.1.5 in terms of q_0 and H_0 but we leave this as an Exercise !.

If we use this expansion in Eqn. 2.27 for the propagation of light we obtain on for left hand side

$$\int_{t_1}^{t_0} \frac{dt}{a(t)} = \frac{1}{a(t_0)} \int_{t_1}^{t_0} \left[1 + H_0(t_0 - t) + \left(1 + \frac{q_0}{2}\right) H_0^2 (t_0 - t)^2 + \cdots\right]$$

and for the right hand side

$$\int_0^{r_1} \frac{dr}{(1 - Kr^2)^{1/2}} \approx \frac{1}{|K|^{1/2}} \int_0^{|K|^{1/2} r_1} \left(1 + \frac{1}{2} k r^{*2}\right) dr^* = r_1 + \mathcal{O}(r_1^3)$$

and we obtain

$$r_1 = \frac{1}{a(t_0)} \left[t_0 - t_1 + \frac{1}{2} H_0 \left(t_0 - t_1\right)^2 + \cdots\right] .$$

Furthermore we obtain for the redshift

$$z = \frac{1}{a} - 1 = H_0(t_0 - t_1) + \left(1 + \frac{q_0}{2}\right) H_0^2 \left(t_0 - t_1\right)^2 + \cdots$$

and hence

$$r_1 = \frac{1}{a(t_0) H_0} \left[z - \frac{1}{2} \left(1 + q_0\right) z^2 + \cdots\right] .$$

Finally we can write the expansion of the luminosity distance for low redshifts

$$d_{\mathrm{L}} = H_0^{-1} \left[z + \frac{1}{2} \left(1 - q_0\right) z^2 + \cdots\right] . \tag{2.38}$$

This expansion will play a vital rôle for the calibration of the magnitude - redshift relation for Supernovae as we will discuss it in Section 2.3.

2.2.4 Volumes

In general the volume element for a 3-space with metric h_{ab} is given by

$$dV = \sqrt{h}\, dx_1 dx_2 dx_3 ,$$

where $h \equiv \det h_{ab}$ is the determinant of the metric[4]. In case of the spatial part of the Robertson-Walker metric from Eqn. 2.10 we obtain for the proper volume element at the coordinates $(t_1, r_1, \theta_1, \phi_1)$

$$dV_p = a^3(t_1)(1 - Kr_1^2)^{-1/2} r_1^2 \sin\theta_1 \, d\phi_1 d\theta_1 dr_1 ,$$

[4]Note that actually the determinant is quite often referred to as the volume form.

where $r_1 = r(t_1)$ with

$$\int_t^{t_0} \frac{dt}{a(t)} \equiv \int_0^{r(t)} \frac{dr}{\sqrt{1-Kr^2}}\,,$$

and hence

$$dr_1 = -\left(1-Kr_1^2\right)^{1/2} \frac{dt_1}{a(t_1)}\,.$$

Therefore

$$dV_p = 4\pi a^2(t_1) r^2(t_1) |dt_1|\,.$$

here dt can be rewritten first in terms of $a(t)$ with $dt = da/(Ha)$ and then with redshift to $dt = -adz/H$ and we obtain,

$$dV_p = 4\pi a^3(t_1) \frac{r_1^2}{H(t_1)} dz$$

and the *comoving volume element* per solid angle

$$\boxed{\frac{dV}{dz d\Omega} = \frac{r^2}{H}\,, \qquad (2.39)}$$

where $r(t)$ can be obtained from Eqn. 2.28.

If we want the overall comoving volume at (t_1, r_1) we have to integrate

$$\frac{dV_p}{a^3} = dV = (1-Kr)^{-1/2} r^2 \sin\theta \; d\phi d\theta dr\,,$$

where the division by a^3 on the left hand side has been performed in order to obtain the comoving volume element. We can then integrate the right hand side easily over the angles. For the r_1 integration we first substitute again $r_1^* = |K|^{1/2} r$ and $K = k|K|$ and obtain

$$V = \frac{4\pi}{|K|^{3/2}} \int_0^{r_1^*} \frac{r^{*2} dr^*}{\sqrt{1-kr^{*2}}}\,.$$

For flat space with $K = 0$ we obtain trivially

$$V = \frac{4\pi}{3} r_1^3\,.$$

For $K > 0$ we substitute $r^* = \sin u$ and obtain

$$V = \frac{2\pi}{|K|^{3/2}} \left[\sin^{-1} r_1^* - r_1^* \sqrt{1-r_1^{*2}}\right]\,.$$

For $K < 0$ we substitute $r_1^* = \sinh u$ and get

$$V = \frac{2\pi}{|K|^{3/2}} \left[-\sinh^{-1} r_1^* + r_1^* \sqrt{1+r_1^{*2}}\right]\,.$$

2.3 Distance vs. Redshift with Type Ia Supernovae

We will now study an application of what we have learned so far. The analysis of the distance - redshift relation with Type Ia Supernovae and the what we can learn about the cosmological parameters H_0, $\Omega_{\Lambda,0}$, $\Omega_{\mathrm{m},0}$ and $\Omega_{\mathrm{k},0}$.

However in order to do this we need to introduce the notion of magnitudes.

2.3.1 Cosmological Magnitudes

When we discussed the luminosity distance in Section 2.2.3 we introduced the notion of of bolometric flux, which is related to the bolometric brightness. The brightness in general is the intensity of a radiating source, ie. the energy flux per solid angle and per unit frequency. The bolometric brightness again is integrated over a frequency wave band. Now the definition of magnitudes is an ancient concept. Hipparchus (150 BC) divided stars into six classes of brightness he called magnitudes. The brightest stars were called first magnitude and the faintest sixth. With quantitative measurements it was found that each jump in magnitude corresponded to a fixed *ratio* in flux, hence the magnitude scale is logarithmic. This is not too surprising since the eye has an approximately logarithmic response to light, which enables a large dynamic range. It was found that a difference of five magnitudes corresponds to a factor 100 in brightness and we have

$$\frac{b}{B} = 100^{(M-m)/5} = 10^{(m_2-m_1)/2.5}\,.$$

Instead of using the brightness ratio we could have also used the ratio of the received flux. We can now build up the magnitude ladder with a standard candle. A standard candle is an object which has always the same emitted luminosity $\mathcal{L}$. We obtain then with Eqn. 2.33

$$M - m = 2.5 \log \frac{d_{\mathrm{L},0}^2}{d_{\mathrm{L}}^2} = 5 \log \frac{d_{\mathrm{L},0}}{d_{\mathrm{L}}}\,,$$

where M is the intrinsic magnitude of the standard candle at some close by distance $d_{\mathrm{L},0}$. In astronomical situations this distance is usually chosen to

$10\,\mathrm{pc}$[5]. So usually one obtains

$$m = M + 5\log d_{\mathrm{L}}\,.$$

where d_{L} is given in units of $10\,\mathrm{pc}$. However in cosmological situation this is a rather small distance and a more natural unit is $1\,\mathrm{Mpc}$. If we measure the distance in this unit the apparent magnitude is given by

$$\boxed{m = M + 5\log d_{\mathrm{L}} + 25\,. \qquad (2.40)}$$

If we use the approximation for $z \ll 1$ for the luminosity distance in Eqn. 2.38 we obtain

$$m = M - 5\log H_0 + 5\log cz + \cdots + 25\,. \qquad (2.41)$$

Note that we explicitly write the speed of light c in this equation. This approximation only depends on the Hubble constant H_0 but not on other cosmological parameters. So nearby objects can be used to calibrate for the intrinsic magnitude M.

2.3.2 Type Ia Supernovae as Standardizable Candles – Phillips Relation

In order to study the magnitude-redshift relation to very large distances, one needs a very bright standard candle. Type Ia Supernovae explosions are a good candidate for such a standard candle. Since Supernovae are almost as bright as their host galaxies they can be observed to large distances. An example how bright these objects are can be seen in Fig. 2.9. Observationally Type I Supernovae are distinct from Type II that they have *no* hydrogen lines in their maximum light spectrum. Additionally Type Ia show a strong Si absorption feature at $6150\mathring{A}$.

Type Ia Supernovae are probably the product of mass being accreted to a white dwarf in a close binary system. A white dwarf is a an approximately earth size star which is only supported by its electron degeneracy pressure (Pauli principle). Chandrasekhar showed that there is an upper mass limit which can be supported by electron degenarcy pressure which is called the Chandrasekhar mass which is

$$M_{\mathrm{Ch}} = 1.44 M_{\odot}\,.$$

[5]The unit 1 pc is defined to be the distance of an object which produces one arcsec of a parallax angle for one astronomical unit (AU), which is the distance from the sun to the earth. $1\ \mathrm{pc} = 3.09 \times 10^{16}$ m.

Figure 2.9: Type Ia Supernovae 1998aq in NGC3982 (picture taken by H. Dahle). This is a spiral galaxy in Ursa Major of visual brightness 11.8 mag. The Supernovae itself was estimated to reach 11.4 mag. The galaxy is at a distance of ≈ 20.5 Mpc (Stetson & Gibson 2001).

Sometimes there is too much mass accreted onto the white dwarf and its starts to exceed the Chandrasekhar mass limit. In this case the degenerate electron pressure can no longer support the star and it collapses. The collapse energy drives nuclear reaction which build up ^{56}Ni which β-decays into ^{56}Co which in turn β-decays into ^{56}Fe.

These thermonuclear explosions lead to typical typical brightening and fading of the Supernovae, which in case of the Type Ia is governed by a two exponential whose timescale is governed by the two β-decays. Note the the β-decay of ^{56}Ni has a halftime of $\tau_{\rm Ni} = 17.6$ days. In Fig. 2.11 we see a typical SNe observation, where the discovery was made from the ground and the follow up with the Hubble Space Telescope. The brightening and fading gives rise to a typical lightcurve for Type Ia Supernovae as shown in Fig. 2.12. One problem with Type Ia SNe is however that, although they have a narrow range of absolute peak magnitudes M, there is a slight variation.

However Phillips (1993) discovered that there is a tight relation between the peak magnitude and the decay time. This relation is not well understood yet from a theoretical point of view but basically the time scale and the

Figure 2.10: Model of close binary system which might be the progenitor to a Type Ia Supernovae explosion [Picture take from Paul Rickers web page].

Figure 2.11: The brightening and fading of SNe 1998ay.

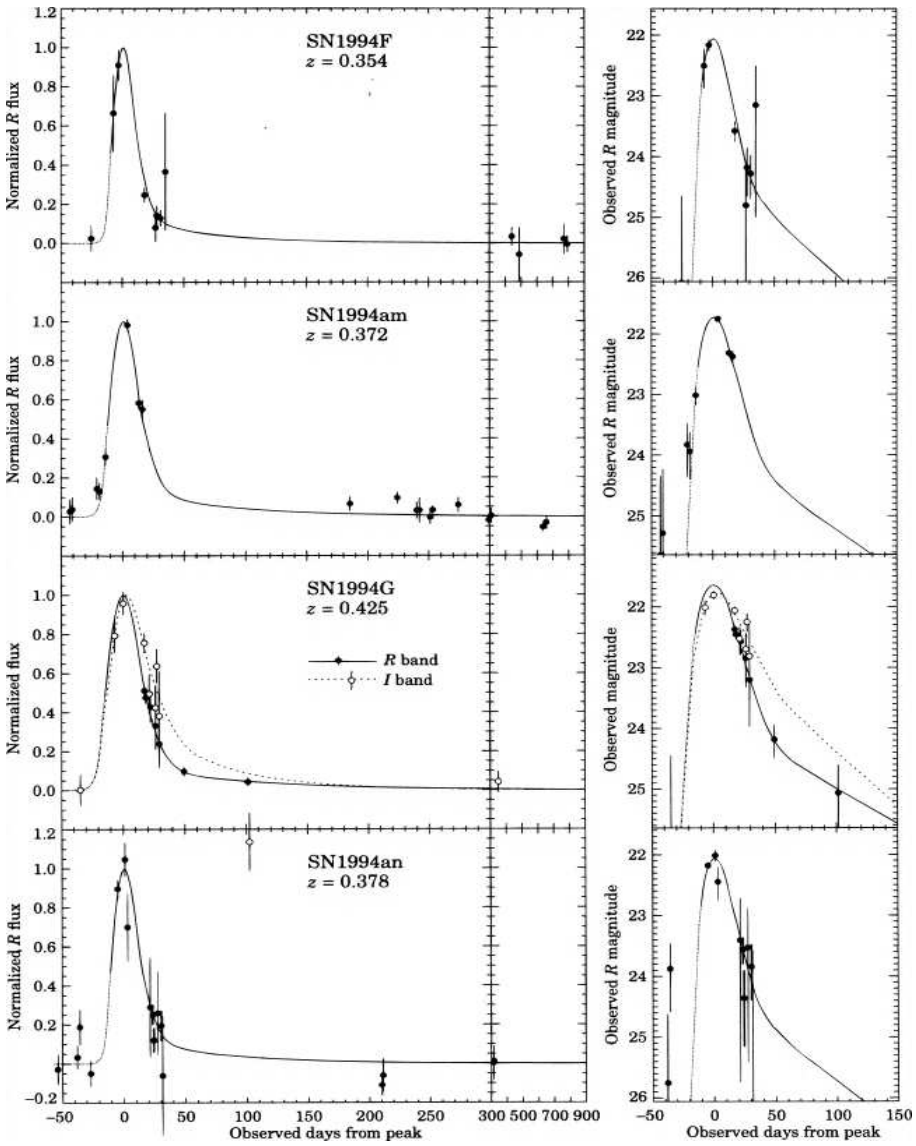

Figure 2.12: Various lightcurves of Type Ia SNe as discussed by Perlmutter et al. (1997).

overall energy of the Supernovae explosion depend both on the amount of Ni which is present in the progenitor. With the Phillips relation it is possible to normalize the peak flux and also "stretch" the time axis so that all Type Ia SNe fit a universal lightcurve. Hence if we know the "intrinsic" , normalized

magnitude of a Type Ia Supernovae and its decay time (sometimes measured as the magnitude after 15 days) we can work out the intrinsic magnitude of this particular SNe. With spectral information of the host galaxy we can work out the redshift of the SNe and hence draw an apparent magnitude - redshift diagram.

If we have a sample of low redshift Type Ia SNe we can use Eqn. 2.41, measure the apparent magnitude and redshift and hence work out

$$\mathcal{M} \equiv m - \log cz = M - 5 \log H_0 + 25 \,, \tag{2.42}$$

which is a measure of the absolute magnitude. If we know this for all SNe we can write

$$m = \mathcal{M} + 5 \log \mathcal{D}_{\rm L} \,, \tag{2.43}$$

with $\mathcal{D}_{\rm L} = H_0 d_{\rm L}$ the Hubble constant free luminosity distance. In Fig. 2.13 we show the measured magnitude redshift relation and some theoretical predications. We see that a flat matter dominated universe (short dashed line) is systematically under-predicting the magnitudes and hence is not a good fit. However the presence of a cosmological constant improves the fit considerably.

2.3.3 Parameter Estimation

In order to quantify which cosmological model fits the data the best we have to address a parameter estimation problem. The topics discussed in this Section apply in general for the estimation of parameters and are hence a valuable tool for every physicist who has to deal with data.

Let us assume that we have a sample of Type Ia SNe with a given magnitude m_i and uncertainty in the magnitude $\sigma_{m,i}$, which is typically of the order $\sigma_m = 0.15$ mag. Furthermore we know the redshift z_i of the Supernovae. In general this redshift has an errorbar as well, but it can be neglected in comparison to the magnitude uncertainty. We can than compare the measurement with the theoretical prediction of Eqn. 2.43 for each set of parameters $(\Omega_{\rm m,0}, \Omega_{\Lambda,0}, \mathcal{M})$. There are two ways to tackle the absolute magnitude $\mathcal{M}$. We could first just look at the low redshift SNe sample from Calan/Tololo and use Eqn. 2.42 to measure the absolute magnitude. Note that this equation does *not* depend on the cosmological parameters. Secondly we could view $\mathcal{M}$ as a free parameter like the cosmological parameters $(\Omega_{\rm m,0}, \Omega_{\Lambda,0})$ and try to find the best fit value for it.

We will follow the second approach here. In order to get a compact notation we define the parameter vector

$$\theta \equiv (\Omega_{\rm m,0}, \Omega_{\Lambda,0}, \mathcal{M}) \,.$$

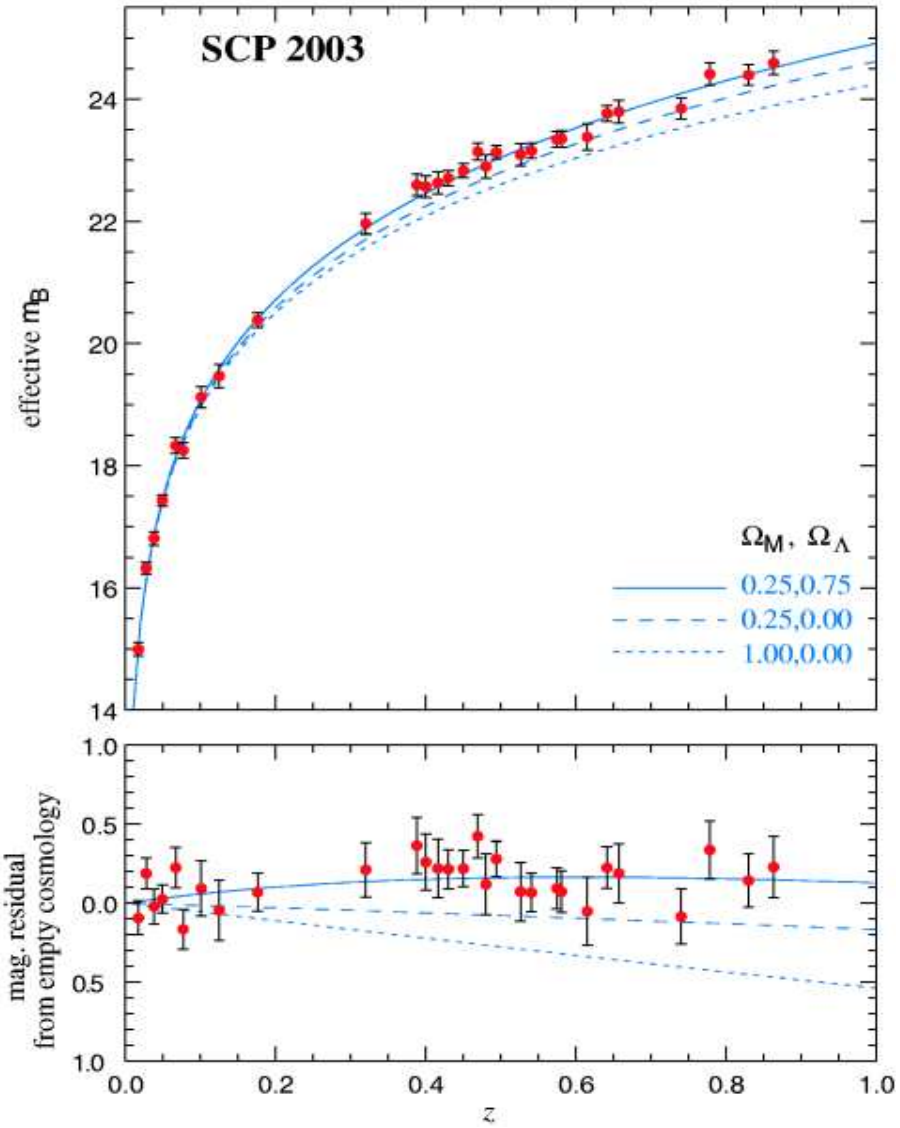

Figure 2.13: Magnitude - Redshift diagram from Knop et al. (2003). The data points are from the Supernovae Cosmology project at high redshifts and from the Calan/Tolo survey at low redshifts. The lower panel shows the relative magnitudes to an empty (Milne) universe with $\Omega_{k,0} = 1$ and $\Omega_{\Lambda,0} = \Omega_{m,0} = 0$.

If we assume that the errors in the magnitude follow a Gaussian distribution we can obtain the best fit parameters by maximising the posterior probability (likelihood)

$$L(\theta) \propto \exp\left[-\frac{1}{2}\chi^2\right]$$

with

$$\chi^2 = \sum_{i=1}^{N} \left(\frac{m(z_i;\theta) - m_i}{\sigma_{m,i}}\right)^2 ,$$

where N is the number of data points. One can then numerically minimize Eqn. 2.3.3 and obtain the best fit values $\hat{\theta}$. As a matter of fact by calculating $L(\theta)$ over the entire sensible parameter range we obtain the posterior distribution[6].

Since from a cosmological point of view we are not interested in the absolute magnitude $\mathcal{M}$ we can marginalize over it and obtain the 2-dimensional probability distribution

$$\tilde{L}(\Omega_{\mathrm{m},0}, \Omega_{\Lambda,0}) = \int d\mathcal{M}\; L(\Omega_{\mathrm{m},0}, \Omega_{\Lambda,0}, \mathcal{M})\,.$$

Fig. 2.14 shows the joint joint likelihood contour where different contours correspond to different likelihood levels. The best fit value is roughly at $\Omega_{\mathrm{m},0} = 0.3$ and $\Omega_{\Lambda,0} = 0.7$, but from a statistical point of view models with in the 68% ($1-\sigma$) or even the 95% ($2-\sigma$) contour are still viable. However even on the 99% level the cosmological constant is positive and non-vanishing. In 1997 Supernovae Cosmology Project and the High-z Supernovae Search team (Perlmutter et al. and Riess et al.) reported similar results, which led to a renewed interest into the cosmological constant. Historically Einstein introduced the cosmological constant in order to balance the gravitational effects of matter and obtain a static universe. After Hubble's discovery that the universe is expanding Einstein abandoned the idea of a static universe and the cosmological constant.

[6]Note that a very efficient way of sampling posterior probabilities is the so called Markov Chain Monte Carlo (MCMC) method. This method randomly selects a parameter set and calculates the likelihood for it. The next parameter set is chosen randomly again. Now this new parameter set is only selected if it fulfils a certain probability criteria, otherwise the previous parameter set is counted twice. This method is iterated and one can show that for a sufficient amount of samples one obtains a good "picture" of the true likelihood. This has advantages over sampling the likelihood just over a gridded parameter space.

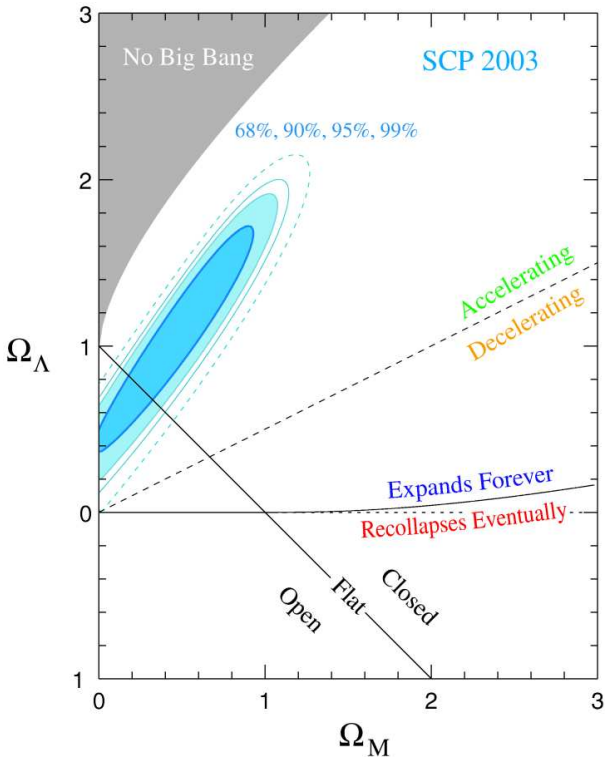

Figure 2.14: Joint likelihood contours in the $\Omega_{m,0} - \Omega_{\Lambda,0}$ plane. The plot is from the Knop et al. (2003) analysis.

Chapter 3

Dark Energy

In order to explain the Type Ia Supernovae data discussed in the previous section 2.3 it is necessary that the expansion of the universe is accelerating. Hence the deceleration parameter q_0 has to be negative.

3.1 Generalized Equation of State

As it is obvious from the discussion in beginning of Section 2.1.5 the cosmological constant can be viewed as another fluid component in the universe, like matter or radiation. If we write the 2nd Friedman equation 2.12 in terms of ρ_Λ and require that it takes the generic form

$$\frac{\ddot{a}}{a} = -\sum_i \frac{4\pi G}{3} \left(\rho_i + 3p_i\right) ,$$

where the summation runs over *all* fluid components we obtain for consistency reasons

$$p_\Lambda = -\rho_\Lambda ,$$

which means the pressure in a cosmological constant fluid is negative. If we use the conservation of energy for this fluid we obtain from Eqn. 2.13

$$\dot{\rho}_\Lambda = -3 \left(\rho_\Lambda + p_\Lambda\right) \frac{\dot{a}}{a} = 0 ,$$

and hence as we see already from the definition of ρ_Λ in Eqn.2.15 that $\rho_\Lambda = \text{const.}$. As a matter of fact we could have started with this and than showed with Eqn. 2.13 that the pressure has to be the negative of the energy density.

Now in general the behaviour of simple fluids (or gases) is governed by their *equation of state*

$$\boxed{p = w\rho\,, \qquad (3.1)}$$

with w the constant equation of state factor. Note that "ordinary" cold dark matter has an equation of state factor $w = 0$, since it is pressureless. Relativistic matter like radiation has a pressure $p = \rho/3$ and hence $w = 1/3$. While as argued before a cosmological constant has an equation of state of $w = -1$.

Let us now explore the question what type of fluid to get accelerated expansion of the universe if we drop the cosmological constant. From Eqn. 2.13 we obtain for a fluid with an equation of state factor w

$$\boxed{\rho_{\rm de}(a) = \rho_{\rm de,0} a^{-3(1+w)}\,, \qquad (3.2)}$$

with $a_0 = 1$ where we introduced the label "de" for *dark energy*. The phrase "dark energy" was coined to describe a component which does not gravitationally clump and has no large interactions with ordinary and cold dark matter. As before we can define the densities in units of the critical density $\rho_{\rm crit}$ and obtain the quantities $\Omega_{\rm de}$ and $\Omega_{\rm de,0}$.

If we assume we have a flat ($K = 0$) universe which has only the dark energy component it is straight forward to show

$$a(t) = \left[\frac{3(1+w)}{2} H_0 t\right]^{\frac{2}{3(1+w)}}$$

where this solution is only valid for $w \neq -1$[1]. From the 2nd Friedmann equation 2.12 we obtain in this case

$$\frac{\ddot{a}_0}{a_0} = -\frac{\Omega_{\rm de,0} H_0^2}{2}\,(1+3w)\,,$$

where $\Omega_{\rm de,0} = 1$ because we assumed $K = 0$. Therefore we obtain for the deceleration parameter from Eqn. 2.37

$$q_0 = -\frac{\ddot{a}_0}{a_0 H_0^2} = \frac{1+3w}{2}$$

[1]Note however that fluids with $w < -1$ are very unphysical since they lead to negative energy densities which are unstable.

and from the condition $q_0 < 0$ for acceleration we obtain $w < -1/3$. If we include a matter component this condition generalises in a flat universe to $w < -1/(3\Omega_{\mathrm{de},0})$ Exercise !.

We can now as described in Section 2.3.3 estimate the best fit values on w, $\Omega_{\mathrm{m},0}$ and $\Omega_{\Lambda,0}$. However for this analysis it is usually assumed the universe is flat and $\Omega_{\Lambda,0} = 1 - \Omega_{\mathrm{m},0}$ is not a free parameter. In Fig. 3.1

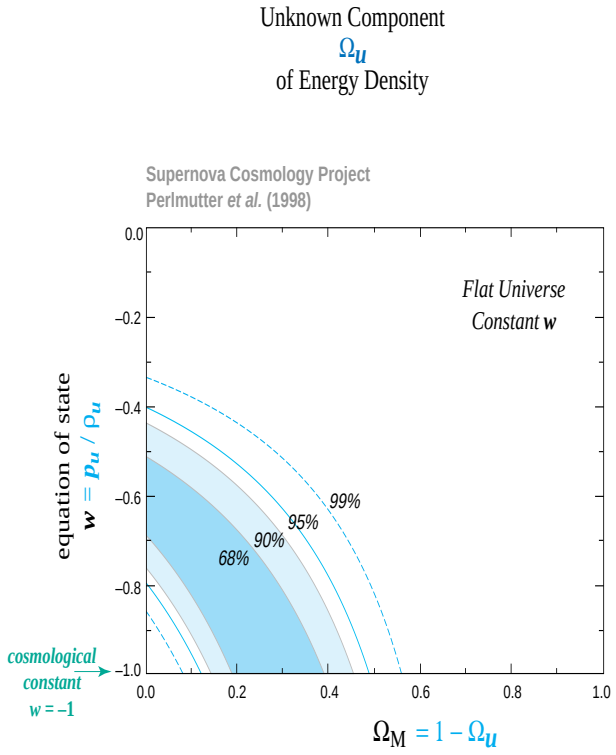

Figure 3.1: Joint likelihood contours in the $\Omega_{\mathrm{m},0} - w$ plane. The plot is from the Perlmutter et al. (1998) analysis for the Supernovae Cosmology Project.

we show the result of the parameter estimation procedure as performed by the SCP collaboration (1998). Again we recognize a non-vanishing $\Omega_{\mathrm{de},0} = 1 - \Omega_{\mathrm{m},0}$ component and a $w < -1/3$ on the 99% level, which is a clear indication that the expansion of the universe is accelerating.

3.2 Scalar Fields and Fine Tuning

In the last Section we have shown that an equation of state for the dark energy component with $w < -1/3$ is sufficient to explain accelerated expansion. For a cosmological constant with $w = -1$ the energy density remains constant over the entire evolution of the universe. One way to interpret the cosmological constant is that it corresponds to an energy of the vacuum. This is can be seen directly from the Einstein equation 2.6, since the presence of Λ leads to a curvature of the universe without the presence of any other energy component. The energy density in the cosmological constant with current measurements is

$$\Omega_\Lambda = 0.7 \rightarrow \rho_\Lambda \approx 10^{-48}\ \text{GeV} \approx 10^{-121}\ M_{\text{pl}}^4\,,$$

where the Planck units are the characteristic scale for the initial conditions of the universe, when the system becomes governed by a still absent theory of quantum gravity[2]. The Planck mass is defined, where the de Broglie wavelength of a particle becomes equal to its Schwarzschild radius

$$\frac{2\pi\hbar}{m_{\text{Pl}}c} = \frac{2Gm_{\text{Pl}}}{c^2}\,.$$

Note that in the notes here it is more convenient to talk in terms of the *reduced* Planck mass

$$\boxed{M_{\text{Pl}} = \sqrt{\frac{\hbar c}{8\pi G}} \approx 2 \times 10^{18}\ \text{GeV}\,, \quad (3.3)}$$

and hence the initial conditions for the cosmological constant need to be fined tuned to a quite unnatural number, which is about 120 (!) orders of magnitude lower than the natural expected value. This is one of the biggest embarrassments of modern cosmology.

Now as mentioned above the cosmological constant can be viewed as the vacuum energy present in the universe. If we believe in supersymmetric fundamental theories there is *no* vacuum energy, which is one of it strength. This is because each fundamental particle has a fermionic or bosonic partner which cancels the vacuum energy exactly to zero. However we know that supersymmetry must be broken at some stage in the universe, because we do not observe it at low energies today. Models for supersymmetry breaking

[2] Although string theory looks as a very promising candidate.

roughly predict a scale of 1 TeV which is still too large to explain the observed values.

Still looking for a field which has a vacuum energy of the cosmological constant might still bring valuable insights. The simplest field we can thin about is a scalar field with the Lagrangian

$$\mathcal{L} = \frac{1}{2}\partial_\mu\phi\partial^\mu\phi - V(\phi)\,,$$

which has the usual form of kinetic minus potential energy, with the action

$$A = \int d^4x\ \sqrt{-g}\mathcal{L}\,.$$

Note the $\sqrt{-g}$ factor is the Jacobian due to the integration over the 4-dimensional space-time volume in the action. Now in order to look at the cosmological consequences we need the energy-momentum tensor for a the scalar field. It can be obtained by applying Noether's theorem[3]. The conserved quantity corresponding to infinitesimal changes in time and space parameters is

$$T_{\mu\nu} = \frac{\partial\mathcal{L}}{\partial(\partial^\nu\phi)}\frac{\partial\phi}{\partial\phi^\mu} - \mathcal{L}g_{\mu\nu}\,.$$

If we assume we have a homogeneous scalar field, which we have to have from a cosmological point of view in order to fulfill the cosmological principle, we can show that in Minkowski space ($g_{\mu\nu} = \eta_{\mu\nu}$) we have for the energy density

$$T_{00} = \rho_\phi = \frac{1}{2}\dot{\phi}^2 + V(\phi) \tag{3.4}$$

and for the momentum density (pressure)

$$T_{ij} = p_\phi = \frac{1}{2}\dot{\phi}^2 - V(\phi)\,. \tag{3.5}$$

From this we see that the equation of state is given by

$$w = \frac{\frac{1}{2}\dot{\phi}^2 - V(\phi)}{\frac{1}{2}\dot{\phi}^2 + V(\phi)}\,.$$

If the kinetic part is much smaller than the potential energy ($\dot{\phi}^2/2 \ll V(\phi)$) the equation of state factor $w \to -1$ if $V \neq 0$. This again stating that a

[3]Noether's theorem is powerful tool which states that each symmetry of the Lagrangian has a corresponding conserved quantity. Symmetry in time results in energy conservation and the homogeneity in space in momentum conservation.

cosmological constant corresponds to a constant vacuum energy. Hence in order to obtain accelerated expansion we need a scalar field whose kinetic energy is negligible compared to the potential[4]. In Fig. 3.2 we see two

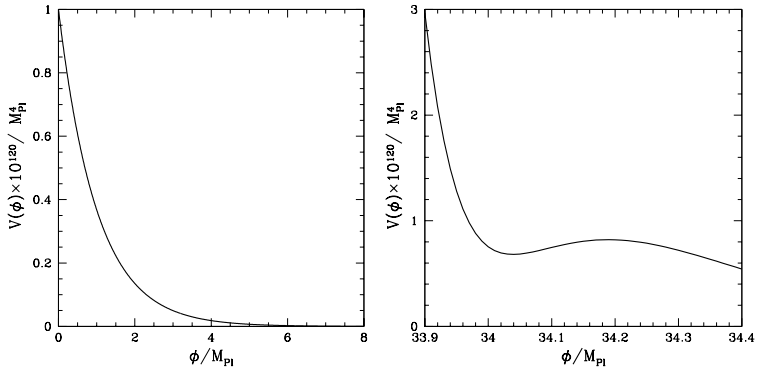

Figure 3.2: Typical potential for scalar field dark energy models (Quintessence). On the left a "slow roll" configuration and on the right a "false vacuum" configuration.

typical potentials for dark energy configurations. On the left is a "slow roll" configuration where the scalar field is still dynamically evolving, but its kinetic energy is negligible compared to the potential. On the right is a configuration where the scalar field is actually frozen in, in a "false vacuum" state (false vacuum, because the "true " vacuum represents the lowest energy state). In general dark energy models with (canonical) scalar field are called *Quintessence* to describe the fifth element character (besides, gravitational, electro-magnetic, weak and strong interactions). Besides of describing a dynamical approach there is hope that these fields can be linked with fundamental theories, like string theory.

3.2.1 The Exponential Potential

One of the earliest studies of scalar fields and their influence on the evolution on the *late* universe, was done in 1988 for an exponential potential (Ratra & Peebles; Wetterich). In general we obtain from the conservation of energy

[4]This is the same requirement as for so called inflationary models, which describe a phase of exponential expansion in the *early* universe. As a matter of fact the dark energy scalar field dark energy models we are going to discuss represent some sort of *late* time inflation.

in Eqn. 2.13

$$\ddot{\phi} + 3H\dot{\phi} + V' = 0\,, \tag{3.6}$$

with the prime denoting the derivative with respect to the field and

$$H^2 = \frac{1}{3M_{\rm Pl}^2}\left(\frac{1}{2}\dot{\phi}^2 + V(\phi) + \rho_n\right)\,, \tag{3.7}$$

Let us start with the simple example where there is *no* other component. We then would like to answer the question if there are any potentials which would lead to an equation of state $p_\phi = w\rho_\phi$ with w constant. By subtracting and adding Eqns. 3.4 and 3.5 we obtain

$$V = \frac{1-w}{2}\rho_\phi$$

and

$$\dot{\phi}^2 = (1+w)\rho_\phi\,.$$

If we then use again Eqn. 3.4 we get

$$\dot{\phi}^2 = 2\frac{(1+w)}{1-w}V$$

and from the time derivative of this equation we obtain

$$\ddot{\phi} = \frac{1+w}{1-w}V'\,,$$

where we have used $\dot{V} = V'\dot{\phi}$. From Eqn. 3.7 with $\rho_n = 0$ we obtain then

$$H^2 = \frac{2V}{3M_{\rm Pl}^2}\frac{1}{1-w}\,.$$

Combining this into the equation of motion, Eqn. 3.6 for the scalar field ϕ we obtain finally

$$2V' + \frac{V}{M_{\rm Pl}}\sqrt{12(1+w)} = 0\,,$$

which is a simple 1st order differential equation we can solve with the ansatz

$$V(\phi) = V_0 e^{-\lambda\phi/M_{\rm Pl}}\,. \tag{3.8}$$

We then obtain

$$\lambda = \sqrt{3(1+w)}\,,$$

and if we require $-1 < w < 1$ we get $\lambda < \sqrt{6}$. With this we can easily obtain the solution for a generic exponential potential $V = V_0 \exp[-\lambda\phi/M_{\rm Pl}]$

$$\begin{aligned} \phi(t) &= \phi_0 + \frac{2M_{\rm Pl}}{\lambda} \ln(tM_{\rm Pl})\,, \\ w &= \frac{\lambda^2}{3} - 1\,, \\ \rho_\phi &\propto a^{-\lambda^2}\,, \\ a &\propto t^{2/\lambda^2}\,. \end{aligned} \tag{3.9}$$

Note that the second last relation is a trivial consequence of $\rho_\phi \propto a^{-3(1+w)}$ for constant w. These are attractor solutions, where small perturbations around it decay like t^{-1} and t^{1-6/λ^2}. To show this is an Exercise ! in the stability of nonlinear differential equations which is beyond the scope of this lecture. For $\lambda > \sqrt{6}$ there is not a single attractor and $\rho_\phi \propto a^{-6}$, with $w \to 1$, which corresponds to kinetic domination of the energy density.

We will now consider the behaviour when a second component with

$$\dot{\rho}_n + nH\rho_n = 0\,,$$

is present, with $n = 3$ ($w = 0$) for matter and $n = 4$ ($w = 1/3$) for radiation with $\rho_n \propto a^{-n}$. There are now two different cases: Those potentials in which the scalar energy density scales slower than a^{-n} ($\lambda < \sqrt{n}$) and those where the scalar energy density scales faster ($\lambda > \sqrt{n}$). Adding an extra component increases the damping term in Eqn. 3.6 and it follows that the scaling in $\rho_\phi \propto 1/a^{\lambda^2-\delta}$ is always slower (than without an extra component ρ_n) with $\lambda^2 \geq \delta \geq 0$. For $\lambda < \sqrt{n}$ the dark energy component scales slower than the other component and will eventually become dominant and reaches the attractor solution in Eqns. 3.9. For $\lambda > \sqrt{n}$ there is a different behaviour. If the field would scale like in the $\rho_n = 0$ case it would be arbitrarily damped (by the present ρ_n component and hence its kinetic energy will be so far reduced that it reaches the $w \to -1$ branch and begins to catch up again and the final behaviour is that the field mimics the dominant component with the attractor

$$\begin{aligned} \Omega_{\rm de} &\equiv \frac{\rho_\phi}{\rho_\phi + \rho_n} = \frac{n}{\lambda^2}\,, \\ \rho_\phi &\propto \frac{1}{a^n}\,, \\ w &= \frac{n}{3} - 1\,. \end{aligned} \tag{3.10}$$

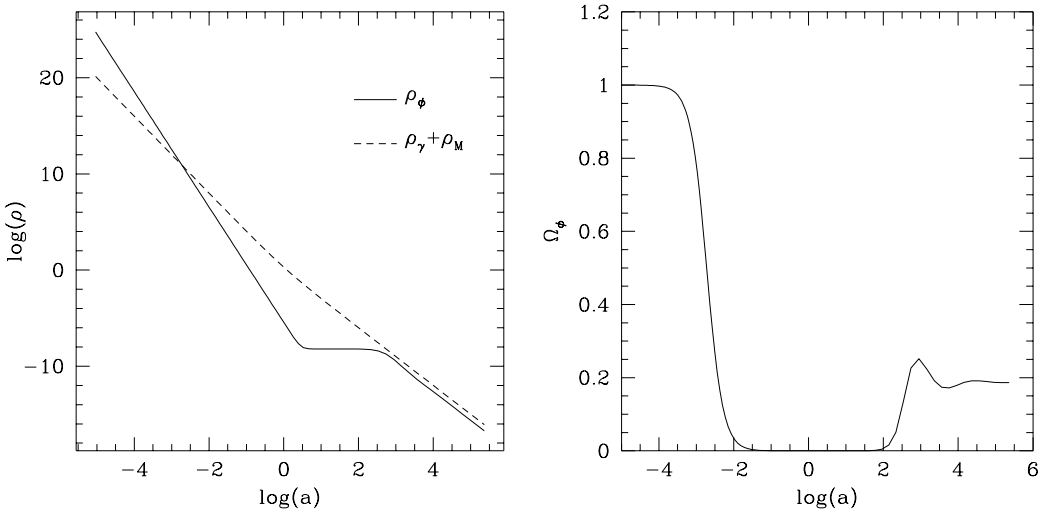

Figure 3.3: Attractor behaviour for exponential dark energy (Ferreira & Joyce 1998). In the left panel we plot the evolution of the energy density in the scalar field (ρ_ϕ) and in a component of radiation-matter as a function of scale factor for a situation in which the scalar field (with $\lambda = 4$) initially dominates, then undergoes a transient and finally locks on to the scaling solution. In the right panel we plot the evolution of the fractional density in the scalar field.

In Fig. 3.3 we show the behaviour for $\lambda = 4$ how the attractor works. Initially the scalar field is domination over radiation and matter and is kinetically dominant and scales like $1/a^6$, until the energy density in radiation is undershot. Then it turns around scaling much slower than radiation or matter until it has caught up and settles down to the fraction given in Eqns. 3.10.

The big advantage of this attractor solutions is that they can start of on an energy scale at early times which is of the order of the Planck scale $\rho_{\phi,i} = \mathcal{O}(M_{\rm Pl}^4)$ and still reaches the attractor. However the attractor given here with $\Omega_{\rm de} = n/\lambda^2$ can *not* explain a universe where the dark energy component dominates. But this is exactly what is required in a flat universe with $\Omega_{\rm de,0} = 0.7$ and $\Omega_{\rm m,0} = 0.3$.

3.3 Tracker Solution

We have seen in the previous Section that although while a exponential potential provides an elegant way to avoid the fine tuning of initial conditions, it unfortunately does not explain why the matter and dark energy density today roughly coincide. One would want that the energy density in the dark energy component somehow tracks below the the other components for most of the evolution of the universe and then suddenly dominates and leads to an accelerated expansion.

The difference of the tracker solutions to the previously discussed exponential potential is that its energy density is changing steadily with ϕ and evtl. manages to overtake the background fields. So we can write down the following two conditions:

(a) As for the self-adjusting exponential potential a wide range of initial conditions should be drawn towards a common cosmic history; but
(b) these tracking solutions should not "self-adjust to th background equation of state, but, instead, maintain some finite difference in the equation-of-state such that the dark energy ultimately dominates and the universe enters a period of acceleration.

Two potentials which fulfill this are

$$V(\phi) = M^{4+\alpha}\phi^{-\alpha}$$

and

$$V(\phi) = M^4 e^{M_{\rm Pl}/\phi}\,,$$

where M is a free parameter which needs to be adjusted in order to obtain $\Omega_{\Lambda,0} = 0.7$ today. The tracker solutions fulfils

$$V'' = (9/2)\left(1-w^2\right)\left[(\alpha+1)/\alpha\right]H^2 \tag{3.11}$$

at all times. Sine ρ_ϕ should begin to dominate today we need ϕ to be $\mathcal{O}(M_{\rm Pl})$ since $V'' \approx \rho_\phi/\phi^2$ and $H^2 \approx \rho_\phi/M_{\rm Pl}^2$. In order to obtain $\Omega_{\Lambda,0} = 0.7$ or $\rho_{\phi,0} \approx 10^{-47}$ GeV we obtain with $V(\phi) \approx \rho_\phi$ imposes the constraint $M \approx (\rho_{\phi,0} M_{\rm Pl}^\alpha)^{1/(\alpha+4)}$. For low values of α the mass M has to be as small as 1 meV. However $M > 1$ GeV - comparable to particle physics scales - is possible for $\alpha \geq 2$. In Fig. 3.4 we show the evolution of the dark energy density and the equation of state for the exponential tracker. If initially ρ_ϕ is smaller than the tracker solution the field remains frozen until H^2 decreases

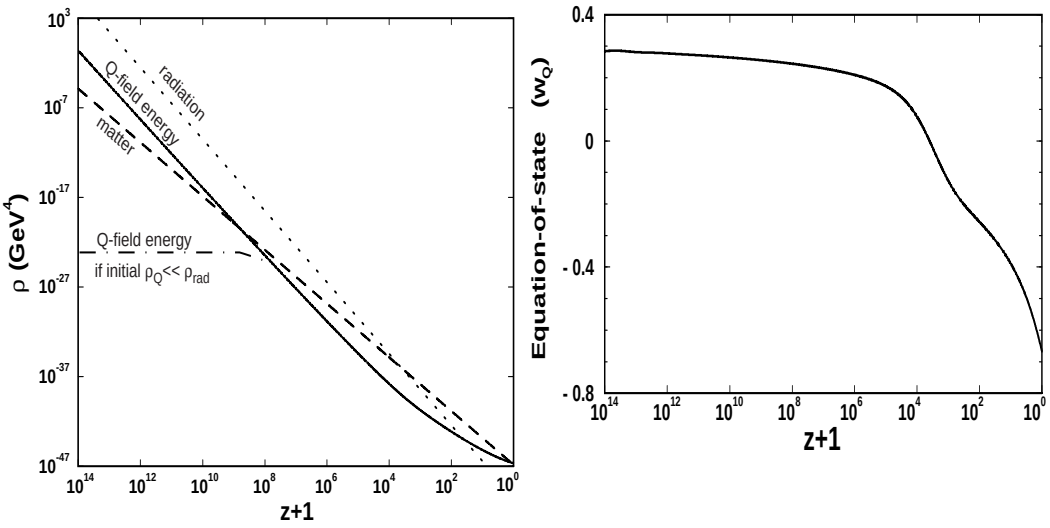

Figure 3.4: Left: Evolution of energy densities for exponential tracker. Right: The evolution of the equation of state [Zlatev et al. 1998].

that the tracker equation 3.11 is fulfilled. Then the field rolls down the potential maintaining Eqn. 3.11. If the energy density ρ_ϕ is larger than the tracker solution, the field starts rolling down the potential immediately and very fast, so that the kinetic energy dominates and shifts as a^{-6} ($w = 1$) until ϕ falls below the tracker and is frozen until it follows it. The equation of state initially is minutely smaller than radiation ($w = 1/3$) and then drops at matter radiation equality below zero and approaches $w \to -1$ when the dark energy becomes to dominate.

To conclude our discussion about dark energy we mention that there is now a plethora of valid dark energy models and we show in Fig. 3.5 the low redshift evolution of the dark energy equation for a sample of models. One of the biggest challenges in modern cosmology is to test which of these models fits the data best and to find out more about the nature of dark energy.

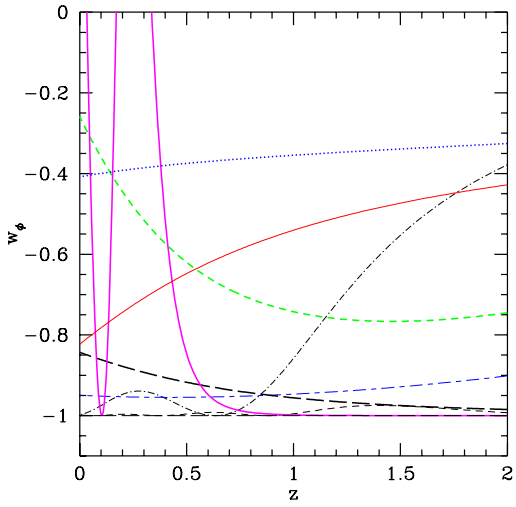

Figure 3.5: Low redshift evolution of the equation of state for a sample of dark energy models [Weller and Albrecht 2001].

Chapter 4

Large Scale Structure

So far we have only studied the large scale evolution of the universe governed by the cosmological principle. However we know that the matter in the universe is *not* distributed entirely homogeneous. An excellent example for this is the recently completed two degree field galaxy redshift survey (2dF) built by the Anglo-Australian observatory, which measure the redshifts of more than 220.000 galaxies

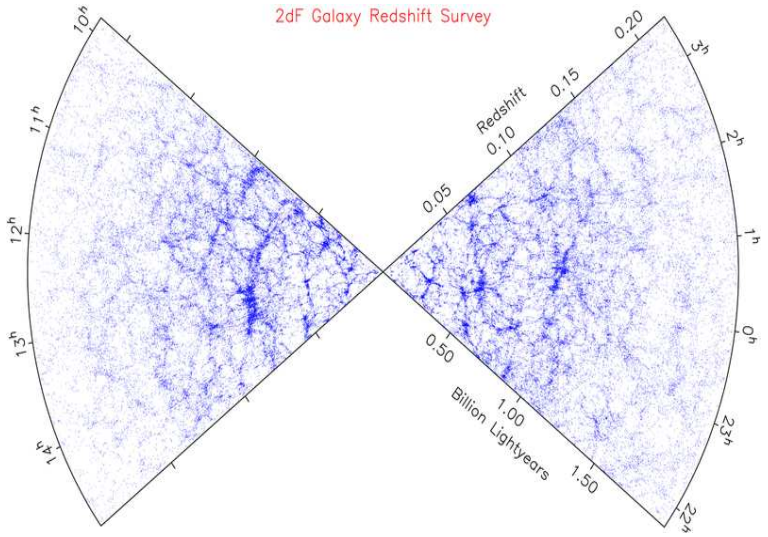

Figure 4.1: Distribution of galaxies as observed by 2dF (2003).

In order to tackle the problem of the distribution of matter in the universe we will first attempt to predict the behaviour of small perturbations

to the smooth background.

4.1 Linear Perturbation Theory

In this Section we will discuss small perturbation to the background fluid. In order to get a better understanding of the effects we will first consider a *Newtonian* fluid before we move on to a full relativistic description.

4.1.1 Non-expanding Newtonian Fluid

As stated in Section 2.1.4 the evolution of a fluid is governed by the Eulerian equations for a perfect fluid

$$\begin{aligned} \frac{\partial \rho}{\partial t} + \nabla \cdot (\rho \mathbf{u}) &= 0 \,, \\ \frac{\partial \mathbf{u}}{\partial t} + (\mathbf{u} \cdot \nabla)\, \mathbf{u} + \frac{1}{\rho} \nabla p + \nabla \Phi &= 0 \,, \\ \nabla^2 \Phi &= 4\pi G \rho \,, \end{aligned} \tag{4.1}$$

where Φ is the gravitational potential and the last equation is the Poisson equation. The trivial solution for this system is $\mathbf{u}_0 = 0$, $\rho_0 = \text{const.}$ and we choose the potential zero point that the gravitational force vanishes $\nabla \Phi_0 = 0$. If we consider perturbations around this static solution

$$\begin{aligned} \rho &= \rho_0 + \delta\rho \\ p &= p_0 + \delta p \\ \mathbf{u} &= \mathbf{u}_0 + \delta \mathbf{u} \\ \Phi &= \Phi_0 + \delta \Phi \,. \end{aligned} \tag{4.2}$$

The pressure and density are related by the equation of state $p = w\rho$. We assume for the moment that there is *no* spatial variation in the equation of state and define the *adiabatic*[1] sound speed

$$\boxed{c_s^2 \equiv \left(\frac{\partial p}{\partial \rho} \right)_{\text{adiabatic}}} \tag{4.3}$$

and since there are *no* spatial variations

$$c_s^2 = \frac{\delta p}{\delta \rho} \,.$$

[1] Note that in general the sound speed of a fluid is $c_s^2 \equiv \delta p / \delta \rho$.

We then obtain from the Euler equations 4.1

$$\begin{aligned} \frac{\partial(\delta\rho)}{\partial t} + \rho_0 \nabla\cdot(\delta\mathbf{u}) &= 0\,, \\ \frac{\partial(\delta\mathbf{u})}{\partial t} + \frac{c_s^2}{\rho_0}\nabla(\delta\rho) + \nabla(\delta\Phi) &= 0\,, \\ \nabla^2(\delta\Phi) &= 4\pi G(\delta\rho)\ , \end{aligned} \tag{4.4}$$

which can be combined to a single 2nd order differential equation for $(\delta\rho)$

$$\ddot{(\delta\rho)} - c_s^2\nabla^2(\delta\rho) = 4\pi G\rho_0(\delta\rho)\ .$$

This is a wave equation with the solution

$$\delta\rho(\mathbf{x},t) = \rho_0\delta(\mathbf{x},t) = A\rho_0\exp\left[-i\mathbf{k}\cdot\mathbf{x} + i\omega t\right]\ , \tag{4.5}$$

with

$$\delta(\mathbf{x},t) \equiv \frac{\delta\rho(\mathbf{x},t)}{\rho_0} \tag{4.6}$$

and ω and $\mathbf{k}$ satisfy the dispersion relation

$$\omega^2 = c_s^2k^2 - 4\pi G\rho_0\,,$$

with $k = |\mathbf{k}|$. If ω is imaginary, there will be exponentially growing (and decaying) modes, while if ω is real the perturbations will oscillate as sound waves. ω is imaginary if k is smaller than some critical value

$$\boxed{k_J \equiv \left(\frac{4\pi G\rho_0}{c_s^2}\right)^{1/2}\ ,} \tag{4.7}$$

which is called the *Jeans* wavenumber. For $k^2 \ll k_J^2$, $\delta\rho$ grows (or decays) exponentially on the dynamical timescale

$$\tau_{\rm dyn} = (\mathrm{Im}\ \omega)^{-1/2} \simeq (4\pi G\rho_0)^{-1/2}\ .$$

It is convenient to define the *Jeans mass*, the total mass contained within a sphere of radius $\lambda_J = \pi/k_J$

$$M_J = \frac{4\pi}{3}(\pi/k_J)^3\rho_0 = \frac{\pi^{5/2}}{6}\frac{c_s^3}{G^{3/2}\rho_0^{1/2}}\,.$$

Perturbations of mass less than M_J are stable against gravitational collapse, while those of mass greater than M_J collapse. The timescale of the gravitational collapse is given by the dynamical timescale $\tau_{\rm dyn}$, while the timescale for the response of the pressure is governed by the size of the perturbation λ divided by the sound speed $\tau_{\rm pressure} \sim \lambda/c_s$. If $\tau_{\rm pressure} > \tau_{\rm dyn}$ there is not enough time for the pressure to oppose the gravitational collapse and the perturbation collapses.

4.1.2 Expanding Newtonian Fluid

Our next step in describing small density perturbations in the Universe is by including the expansion. In this case the unperturbed matter solution is given by

$$\rho_0 = \rho_{\rm m,0} a^{-3}(t)\,, \qquad \mathbf{u}_0 = \frac{\dot{a}}{a}\mathbf{x}\,, \qquad \nabla\Phi_0 = \frac{4\pi G\rho_0}{3}\mathbf{x}\,,$$

where $a(t)$ is the scale factor as usual. Note that this perturbation analysis here is still not in a general relativistic context and is only valid for perturbations on scales smaller than the size of the universe $|\mathbf{x}| < H^{-1}$. The first order perturbation equations are then

$$\begin{aligned} \frac{\partial\left(\delta\rho\right)}{\partial t} + 3\frac{\dot{a}}{a}\left(\delta\rho\right) + \frac{\dot{a}}{a}\left(\mathbf{x}\cdot\nabla\right)\left(\delta\rho\right) + \rho_0\nabla\cdot\left(\delta\mathbf{u}\right) = 0\,, \\ \frac{\partial\left(\delta\mathbf{u}\right)}{\partial t} + \frac{\dot{a}}{a}\left(\delta\mathbf{u}\right) + \frac{\dot{a}}{a}\left(\mathbf{x}\cdot\nabla\right)\left(\delta\mathbf{u}\right) + \frac{c_s^2}{\rho_0}\nabla\left(\delta\rho\right) + \nabla\left(\delta\Phi\right) = 0\,, \\ \nabla^2\left(\delta\Phi\right) = 4\pi G\left(\delta\rho\right)\,. \end{aligned} \tag{4.8}$$

If we introduce the Fourier transform

$$\Psi(\mathbf{x},t) = \frac{1}{(2\pi)^{3/2}}\int \Psi_k(t)\exp\left[\frac{-i\mathbf{k}\cdot\mathbf{x}}{a(t)}\right]\,d^3r$$

and perform this for the quantities $\Psi = \delta, \delta\mathbf{u}, \delta\Phi$ with $\delta = \delta\rho/\rho_0$ we obtain

$$\begin{aligned} \dot{\delta}_k - \frac{i\mathbf{k}}{a}\cdot\delta\mathbf{u}_k = 0\,, \\ \frac{d\left(a\delta\mathbf{u}_k\right)}{dt} - i\mathbf{k}c_s^2\delta_k - i\mathbf{k}\delta\Phi_k = 0\,, \\ \delta\Phi_k = -\frac{4\pi G\rho_0}{k^2}a^2\delta_k\,. \end{aligned} \tag{4.9}$$

It is useful to decompose the perturbed velocity field in rotational ($\mathbf{u}_\perp$) and irrotational modes ($\mathbf{u}_\parallel$)

$$\delta\mathbf{u} = \mathbf{u}_\perp + \mathbf{u}_\parallel\,, \qquad \delta\mathbf{u}_k = \mathbf{u}_\perp\left(\mathbf{k}\right) + \mathbf{u}_\parallel\left(\mathbf{k}\right)\,,$$

with

$$\begin{aligned} \nabla \cdot \mathbf{u}_\perp &= 0\,, & \nabla \times \mathbf{u}_\parallel &= 0\,, \\ \mathbf{k} \cdot \mathbf{u}_\perp(\mathbf{k}) &= 0\,, & \mathbf{k} \cdot \mathbf{u}_\parallel(\mathbf{k}) &= |\mathbf{k}||\mathbf{u}_\parallel(\mathbf{k})|\,, \end{aligned} \tag{4.10}$$

and hence the first order equations become

$$\begin{aligned} \frac{d\left[a\mathbf{u}_\perp(\mathbf{k})\right]}{dt} = 0 \;\Rightarrow\; \mathbf{u}_\perp &\propto a^{-1}(t)\,, \\ \mathbf{u}_\parallel(\mathbf{k}) &= \frac{a}{ik}\dot{\delta}_k + \frac{\mathbf{const}}{a(t)}\,, \\ \ddot{\delta}_k + 2\frac{\dot{a}}{a}\dot{\delta}_k + \left(\frac{c_s^2 k^2}{a^2} - 4\pi G\rho_0\right)\delta_k &= 0\,. \end{aligned} \tag{4.11}$$

We notice that the rotational modes are not coupled to the density perturbations and decay as a^{-1}. From here on we will hence only be interested in irrotational modes and drop the index $\parallel$. Also we will always work in Fourier space and drop the index k. Note that from the equation for δ we recover the previous result if we neglect the expansion ($\dot{a} = 0$) and identify $|\mathbf{k}|/a$ with the physical wavenumber and hence $\mathbf{k}$ is the *comoving* wavenumber. Similar to the previous section the Jeans wavenumber

$$k_J^2 \equiv \frac{4\pi G\rho_0 a^2}{c_s^2}$$

separates gravitationally stable and unstable modes. For short-wavelength modes, $k \gg k_J$ the perturbations oscillate as a sound wave with approximately

$$\omega \approx \frac{c_s k}{a(1-n)}\,,$$

where we assume $a \sim t^n$. In general the exact solution is given by a Bessel function and the amplitude of the soundwave slowly decreases because of the expansion of the Universe. For $k \ll k_J$ there are unstable growing modes. If we assume that the Universe is flat ($K = 0$) , matter dominated with $\dot{a}/a = (2/3)t^{-1}$ and $\rho_0 = (6\pi G t^2)^{-1}$ we obtain

$$\ddot{\delta} + \frac{4}{3t}\dot{\delta} - \frac{2}{3t^2}\delta = 0\,,$$

where we exploited that the pressure gradient is negligible in this limit ($c_s^2 k^2/a^2 \ll 4\pi G\rho_0$). This equation has two independent solutions, a growing mode, δ_+ and a decaying mode δ_- with time dependence given by

$$\delta_+(t) = \delta_+(t_i)\left(\frac{t}{t_i}\right)^{2/3}$$

and

$$\delta_-(t) = \delta_-(t_i)\left(\frac{t}{t_i}\right)^{-1},$$

where t_i is a convenient time chosen for the normalization of the modes. Here we see the effect of the expansion of the universe. The expansion of the Universe slows the otherwise exponential growth of the perturbation and results in a power-law growth for the unstable modes. We note that for the long term evolution only the growing mode is relevant, which will begin to dominate any general solution.

In general the Universe consists of multiple components. This will influence the evolution of the perturbations in the non-relativistic component i by

$$\ddot{\delta}_i + 2\frac{\dot{a}}{a}\dot{\delta}_i + \left[\frac{c_{s,i}^2 k^2}{a^2}\delta_i - 4\pi G\rho_{\rm tot}\sum_j \epsilon_j\delta_j\right] = 0\,, \tag{4.12}$$

with $\epsilon_j \equiv \rho_j/\rho_{\rm tot}$ the fraction of mass in species j.

Let us consider a two component fluid consisting of baryons and photons in the radiation dominated era. In this case $\dot{a}/a = 1/2t$. If we look at the unstable modes ($k \ll k_J$) assume that the photons are smooth ($\delta_\gamma = 0$) and $\epsilon_b \ll 1$, we obtain

$$\ddot{\delta}_b + \frac{1}{t}\dot{\delta}_b = 0\,.$$

The solution in this case is

$$\delta_b(t) = \delta_b(t_i)\left[1 + A\ln(t/t_i)\right]$$

and only a perturbation with initial $\delta_b(t_i)$ can grow and if so very slow.

Next consider a perturbation during a curvature dominated epoch. When the Universe is curvature dominated $4\pi G\rho_{\rm tot} = \frac{3}{2}\rho_{\rm tot}(t)/\rho_{\rm crit}(t) \ll t^{-2}$ and we obtain

$$\ddot{\delta}_b + \frac{2}{t}\dot{\delta}_b + \frac{3}{2t^2}\frac{\rho_{\rm tot}(t)}{\rho_{\rm crit}(t)}\delta_b \simeq \ddot{\delta}_b + \frac{2}{t}\dot{\delta} = 0\,.$$

In this case the solution is

$$\delta_b(t) = A + Bt^{-1}$$

and small perturbations cease to grow and decay. Hence the growth of perturbations in a non-relativistic component during the radiation of curvature dominated epochs is inhibited. The reason for this is simple. In a Universe which is radiation or curvature dominated the expansion is faster as it

would be if only matter is present and the growth of perturbations is further moderated compared to the exponential growth in a non-expanding fluid.

We will now draw our attention to a fluid which consists just out of baryons and photons. The energy density in photons (radiation)is give by the Stefan-Boltzmann law with

$$\rho_\gamma = \frac{\pi^2}{15} T^4 \,,$$

where T is the temperature of the black body. First we consider the Jeans' mass of the baryons in the radiation era, i.e. before electrons and protons recombine to neutral hydrogen. In this phase the baryons and photons are tightly coupled and the pressure provided by the photons leads to the adiabatic sound speed

$$c_s^2 = \frac{1}{3}$$

and we obtain for the physical Jeans' wavenumber

$$k_{\mathrm{J-phys}} = \frac{k_J}{a(t)} = \left(\frac{4\pi G \rho_{\mathrm{tot}}}{c_s^2} \right)^{1/2} = \left(\frac{4\pi^3}{5} \right)^{1/2} \frac{T^2}{m_{\mathrm{Pl}}}$$

which leads to the physical Jeans' mass in *baryons* in the pre-recombination era

$$M_{\mathrm{B-J}} = \frac{4\pi}{3} \rho_{\mathrm{B}} \left(\frac{\pi}{k_{\mathrm{J-phys}}} \right)^3 \simeq 5.4 \times 10^{18} (\Omega_{\mathrm{B},0} h^2) T_{\mathrm{eV}}^{-3} M_\odot \,.$$

Let us assume that the size of the universe (horizon) is $d_H = c/H \sim t$. We obtain then for the baryonic mass inside the horizon

$$M_{\mathrm{B-HOR}} \equiv \frac{4\pi}{3} \rho_{\mathrm{B}} d_H^3 = \frac{t^3}{(\pi / k_{\mathrm{J-phys}})^3} M_{\mathrm{J-B}} \,.$$

In the radiation dominated era we obtain from the 1st Friedmann equation $t^{-1} = (32\pi G \rho_{\mathrm{tot}}/3)^{1/2})$ and we obtain

$$\frac{\pi}{k_{\mathrm{J-phys}}} = \left(\frac{8}{3} \right)^{3/2} \pi c_s t \,,$$

the baryon Jeans mass can then be written in terms of the baryon mass within the horizon

$$\frac{M_{\mathrm{B-J}}}{M_{\mathrm{B-HOR}}} = \left(\frac{8}{3} \right)^{3/2} (\pi c_s)^3 \simeq 26 \,.$$

So during radiation domination the baryonic Jeans mass is larger than the mass within the horizon and if there are unstable modes they can not be treated within the Newtonian analysis.

After recombination matter decouples from radiation. The pressure support is only provided by non-relativistic hydrogen atoms, and the sound speed is

$$c_s^2 = \frac{5}{3}\frac{T_\mathrm{B}}{m}\,,$$

where T_B is the temperature of the baryons and m the mass. After decoupling from the photons the temperature of the baryons scales as a^{-2} (instead of a^{-1}), and we obtain for the baryon temperature after recombination

$$T_\mathrm{B} = \frac{a_\mathrm{rec}}{a}T = \frac{T^2}{T_\mathrm{rec}}\,.$$

This results in the Jeans mass

$$M_{\mathrm{B-J}} \simeq 1.3\times 10^5 (\Omega_{\mathrm{B},0}h^2)^{-1/2}\left(\frac{z}{1100}\right)^{3/2} M_\odot\,,$$

with $M_\odot \approx 2\times 10^{30}$ kg the solar mass. We recognize that now the Jeans' mass is much smaller than in the radiation dominated era, because of the enormous decrease in pressure due to the decoupling of photons and baryons. Hence, before recombination baryons can not form structures and only afterwards sub-horizon overdensities begin to grow.

So far we have treated the photon-baryon fluid as perfect fluid. However during recombination this assumption breaks down. During decoupling the photon mean free path grows, $\lambda_\gamma = (n_e\sigma_T)^{-1}$, and the photons can diffuse out of overdense regions into under-dense regions and hence smoothing the inhomogeneities of the photon-baryon fluid. An exact treatment requires the use of the Boltzmann equation and is part of the proper calculation of cosmic microwave background anisotropies.

4.1.3 Fluctuations in General Relativity

So far our analysis has been Newtonian. For modes well within the horizon $\lambda_\mathrm{Phys} \ll H^{-1}$ this is sufficient. For larger scales the Newtonian expansion velocity exceeds c and the analysis is not valid.

To obtain a simple geometric picture we analyse perturbations of a flat ($K=0$) FRW model

$$H^2 = \frac{8\pi G}{3}\rho_0\,,$$

with $\rho_0 = \rho_{\rm tot} = \rho_{\rm crit}$. If we now consider a model with the same expansion rate H but a density $\rho_1 > \rho_0$

$$H^2 = \frac{8\pi G}{3}\rho_1 - \frac{K}{a^2}\,,$$

with $K > 0$. Note that if the Hubble expansion is these models is equal we obtain

$$\delta \equiv \frac{\rho_1 - \rho_0}{\rho_0} = \frac{K/a^2}{8\pi G\rho_0/3}\,. \tag{4.13}$$

The evolution of δ is hence related to the evolution of the curvature K/a^2 relative to the density ρ_0. In a matter dominated universe $\rho_0 \propto a^{-3}$ and in a radiation dominated universe $\rho_0 \propto a^{-4}$ and hence

$$\delta \propto \frac{a^{-2}}{\rho_0} \propto \begin{cases} a^2 & \text{radiation domination} \\ a & \text{matter domination} \end{cases} \tag{4.14}$$

If we use $a \propto t^{2/3}$ for a matter dominated universe and $a \propto t^{1/2}$ in a radiation dominated universe we get

$$\delta = \delta_i \begin{cases} t/t_i & \text{radiation domination} \\ (t/t_i)^{2/3} & \text{matter domination} \end{cases} \tag{4.15}$$

We will now start our relativistic analysis by introducing the perturbed FRW metric

$$g_{\mu\nu} = g^0_{\mu\nu} + h_{\mu\nu}$$

where $h_{\mu\nu}$ is a *small* perturbation to the metric. We choose the synchronous gauge $h_{00} = h_{i0} = 0$, ie. the perturbations are only in the spatial part, which is achieved by choosing appropriate equal time slices. This does by no means exhaust all of the gauge freedom. If we are only interested in large scales; micro-physical perturbations to the stress energy tensor can be ignored and the perturbations is simply described by $\rho = \rho_0 + \delta\rho$, $p = p_0 + \delta p$ and $u^\mu = u^\mu_0 + \delta u^\mu$. In this instance we will again assume that the equation of state is constant everywhere. We than must solve the perturbed Einstein equation

$$\delta R_{\mu\nu} - \frac{1}{2}\delta[g_{\mu\nu}R] = 8\pi G\delta T_{\mu\nu}\,,$$

or equivalent

$$\delta R_{\mu\nu} = 8\pi G\delta T_{\mu\nu} - 4\pi G\delta[g_{\mu\nu}\mathcal{T}]\,,$$

with $\mathcal{T}$ the trace of the energy-momentum tensor

$$\mathcal{T} = \rho - 3p = (\rho_0 - 3p_0) + (\delta\rho - 3\delta p)\,.$$

For solving the perturbed Einstein equations we first have to calculate the Christoffel connection $\delta\Gamma^{\mu}_{\nu\alpha}$ to first order in $h_{\mu\nu}$. For the unperturbed FRW metric we have $\Gamma^0_{ij} = -(1/2)\partial g_{ij}\partial t$ Exercise ! and hence

$$\delta\Gamma^0_{ij} = -\frac{1}{2}\frac{\partial h_{ij}}{\partial t}\,.$$

We further have to calculate $\delta R_{\mu\nu}$ to first order in $h_{\mu\nu}$ and obtain for example

$$\delta R_{00} = \frac{1}{2}\ddot{h} + \frac{\dot{a}}{a}\dot{h}\,,$$

where we defined

$$h \equiv h^{\mu}_{\mu} = h^{k}_{k} = -\sum_{k=1}^{3}\frac{h_{kk}}{a^2}$$

as the trace of the metric perturbation. For the unperturbed FRW metric one obtains $R_{00} = -3(\ddot{a}/a)g_{00}$. If we calculate the energy-momentum perturbation to first order we obtain

$$\delta T_{\mu\nu} = -\delta p g^0_{\mu\nu} + (\delta\rho + \delta p)u_{0\mu}u_{0\nu} - p_0 h_{\mu\nu} + (\rho_0 + p_0)(u_{0\mu}\delta u_{\nu} + \delta u_{\mu}u_{0\nu})$$

and

$$\delta[g_{\mu\nu}\mathcal{T}] = g^0_{\mu\nu}\,(\delta\rho - 3\delta p) + h_{\mu\nu}\,(\rho_0 - 3p_0)\;.$$

We then obtain three equations, one for the (00), one for the (ij) and one for the $(0i)$ component. The (00) component is then

$$\ddot{h} + 2H\dot{h} = 8\pi G\,(\delta\rho + 3\delta p)\;. \tag{4.16}$$

As when analysing solutions for the FRW models it is useful to exploit the energy-momentum conservation $\partial_\nu T^{\mu\nu} = 0$ instead of one of the field equations. To 1st order this equation is

$$\dot{\delta\rho} + 3H(\delta\rho + \delta p) + (\rho_0 + p_0)\left[-\frac{\dot{h}}{2} + \nabla\cdot\delta\mathbf{u}\right] = 0\,.$$

The metric tensor can always be decomposed in its trace, a transverse traceless and a vectorial piece and the spatial (and only non-vanishing part in synchronous gauge) of the perturbed metric can be written as

$$h_{ij} = h\frac{\delta_{ij}}{3} + h^{\parallel}_{ij} + h^{\perp}_{ij} + h^{T}_{ij}\,,$$

where we decomposed the vectorial part further into a transverse (rotational), $h_{ij}^{\perp}$, and longitudinal (irrotational) part, $h_{ij}^{\parallel}$.

We will concentrate in this lecture on the scalar perturbations but note that the traceless tensor part corresponds to a perturbation like a gravitational wave and the vectorial perturbations couples to the rotational part of the matter velocity $d\mathbf{u}$ and decays like in the Newtonian approach. For the remaining scalar perturbations we obtain in Fourier space

$$\begin{aligned} \ddot{h} + 2H\dot{h} - 3H^2\left(1+3c_s^2\right)\delta = 0\,, \\ \dot{\delta} + (1+p_0/\rho_0)\left(\theta - \dot{h}/2\right) + 3H(c_s^2 - p_0/\rho_0)\delta = 0\,, \\ \dot{\theta} + (2-3c_s^2)H\theta - \frac{k^2 c_s^2}{a^2(1+p_0/\rho_0)}\delta = 0\,, \end{aligned} \tag{4.17}$$

with

$$\theta \equiv \nabla \cdot \delta\mathbf{u} = -i\mathbf{k}\delta\mathbf{u} \tag{4.18}$$

and as usual $\delta = \delta\rho/\rho$. If we assume the perturbation is adiabatic with $p_0/\rho_0 = c_s^2 \equiv \delta p/\delta\rho$, define $\varphi \equiv \theta/H$ and use $y = \ln a$ as the time variable we obtain

$$\begin{aligned} h'' + \frac{1}{2}\left(1-3c_s^2\right)h' - 3\left(1+3c_s^2\right)\delta = 0\,, \\ \delta' + (1+c_s^2)(\varphi - h'/2) = 0\,, \\ \varphi' - \frac{1}{2}\left(9c_s^2 - 1\right)\varphi = 0\,, \end{aligned} \tag{4.19}$$

where the prime denotes $d/dy = H^{-1}d/dt$. Note that we have neglected the last term in Eqn. 4.17 because we want to focus on super horizon modes in this section. This set of equations is equivalent to a single 4th order equation and we expect four independent solutions. Note that there are only two physical modes like in the Newtonian analysis and the other two correspond to the remaining gauge freedom in the synchronous gauge.

In order to solve Eqns. 4.19 we use the ansatz

$$\left[\delta, \varphi, h, h'\right] \propto \chi_i t^{\lambda_i}\,,$$

where χ_i is a 4-dimensional vector. We then can easily find the solutions $\lambda_1 = 0$, $\lambda_2 = -1$, $\lambda_3 = (2+6c_s^2)/(3+3c_s^2)$ and $\lambda_4 = (9c_s^2-1)/(3+3c_s^2)$ with the χ_i

$$\chi_1 \;=\; [0,0,1,0]\,,$$

$$
\begin{aligned}
\chi_2 &= [(1+c_s^2)/2, 0, 1, -3(1+c_s^2)/2]\,, \\
\chi_3 &= [(1+c_s^2)/2, 0, 1, (1+3c_s^2)/2]\,, \\
\chi_4 &= [c_s^2(1+c_s^2)(9c_s^2-1), (3c_s^2+1/2)(1-c_s^2)(9c_s^2-1), \\
&\quad 2(1+3c_s^2)(1+c_s^2), (1+3c_s^2)(1+c_s^2)(9c_s^2-1)]\,. \qquad (4.20)
\end{aligned}
$$

The first two modes are pure gauge modes and we obtain for the growing and decaying modes in the matter dominated era ($c_s^2 = 0$)

$$\delta_+(t) = \delta_+(t_i)(t/t_i)^{2/3}\,, \qquad \delta_-(t) = \delta_-(t_i)(t/t_i)^{-1/3}$$

and for a radiation dominated universe ($c_s^2 = 1/3$)

$$\delta_+(t) = \delta_+(t_i)(t/t_i)\,, \qquad \delta_-(t) = \delta_-(t_i)(t/t_i)^{1/2}\,.$$

Note that the growing mode solutions are the same as for the expanding Newtonian fluid.

To illustrate the gauge modes we look at a solution with $\delta = \varphi = 0$ and define h_{ij} in terms of derivatives of a vector field $\xi(\mathbf{x})$ with

$$h_{ij}(\mathbf{x}, t) = a^2(t)\left[\partial_j \xi_i + \partial_i \xi_j\right]\,. \qquad (4.21)$$

Consider now a coordinate transformation $x^\mu \to x'^\mu = x^\mu - \epsilon^\mu(x)$. For small ϵ^μ the new metric is

$$
\begin{aligned}
g'_{\mu\nu}(x) &= g_{\mu\nu}(x) + g_{\lambda\nu}(x)\frac{\partial \epsilon^\lambda(x)}{\partial x^\mu} + g_{\lambda\mu}(x)\frac{\partial \epsilon^\lambda(x)}{\partial x^\nu} \\
&\quad + \frac{\partial g_{\mu\nu}(x)}{\partial x^\lambda}\epsilon^\lambda(x) + \cdots \\
&= g_{\mu\nu}(x) + \partial_\nu \epsilon_\mu + \partial_\mu \epsilon_\nu\,. \qquad (4.22)
\end{aligned}
$$

Hence the solution in Eqn. 4.21 merely represents a coordinate transformation. The gauge modes discussed above correspond in a similar, but more complicated way, to a coordinate transformation.

4.2 The Power Spectrum - Statistics of Density Fluctuations

We developed now the tools to calculate the evolution density perturbations in different cosmological models. However to compare with observations we are often interested in the statistics of this density field. The first non-trivial quantity is the second moment of the density field given by

$$\xi(\mathbf{r}) \equiv \langle \delta(\mathbf{x})\delta(\mathbf{x}+\mathbf{r}) \rangle \ , \qquad (4.23)$$

which is called the *correlation function*. The angular brackets refer to averaging over the volume V. Since the density perturbation is real we can then

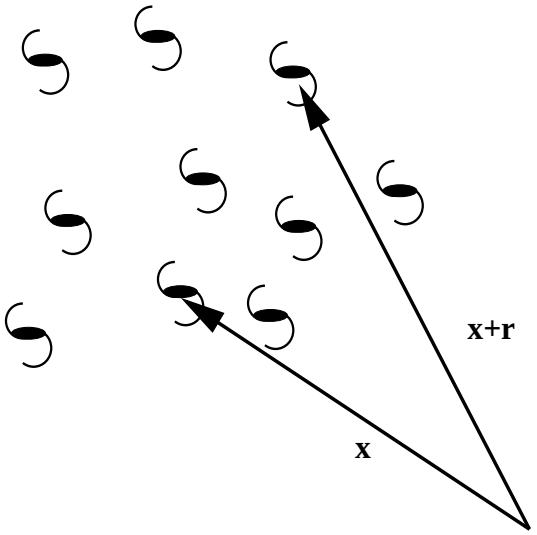

Figure 4.2: Density correlation measurement.

use the Fourier transform of the density field to obtain

$$\xi = \left\langle \frac{V}{(2\pi)^3} \int dk^3 \int dk'^3 \delta_{\mathbf{k}} \delta^*_{\mathbf{k}'} e^{i(\mathbf{k}'-\mathbf{k})\cdot\mathbf{x}} e^{-i\mathbf{k}\cdot\mathbf{r}} \right\rangle$$

and we obtain

$$\xi(\mathbf{r}) = \frac{V}{(2\pi)^3} \int |\delta_{\mathbf{k}}| e^{-i\mathbf{k}\cdot\mathbf{r}} d^3k \qquad (4.24)$$

and we define the power spectrum

$$P(k) \equiv \left\langle |\delta_k|^2 \right\rangle \qquad (4.25)$$

We can now go ahead and define the *isotropic power spectrum* with $< |\delta_{\mathbf{k}}|^2(k) >= |\delta_k|^2(k)$. We further define polar coordinates along the k-axis for the integration in Eqn. 4.24. Since ξ is real it is sufficient to use

$e^{-i\mathbf{k}\cdot\mathbf{r}} \to \cos(kr\cos\theta)$ and we obtain

$$\xi(r) = \frac{V}{(2\pi)^3}\int dk k^2 \int_0^{2\pi} d\phi \int_{-1}^{1} d(\cos\theta) P(k)\cos(kr\cos\theta) = \frac{V}{(2\pi)^3}\int P(k)\frac{\sin kr}{kr} 4\pi k^2 dk\,.$$

Sometimes it is convenient to express the variance per logarithmic k interval ($\Delta^2(k) = d < \delta^2 > /d\ln k \propto k^3 P[k]$):

$$\boxed{\Delta^2(k) \equiv \frac{V}{(2\pi)^3} 4\pi k^3 P(k) = \frac{2}{\pi} k^3 \int_0^\infty \xi(r)\frac{\sin kr}{kr} r^2 dr\,.} \tag{4.26}$$

This is easier to interpret, since $\Delta^2(k) = 1$ means that there are order unity density fluctuations from modes around the logarithmic bin around wavenumber k.

From inflationary models one can motivate he expectation of a featureless power spectrum with

$$\boxed{\left\langle |\delta_k|^2 \right\rangle \propto k^n\,,} \tag{4.27}$$

where n the spectral index governs the power between large and small-scale power. If we measure the power inside a box of comoving length x we obtain

$$\left\langle \delta^2 \right\rangle \propto \int_0^{1/x} k^n 4\pi k^2\, dk \propto x^{-(n+3)}$$

and in terms of mass $M \propto x^3$ we can write

$$\delta_{\rm rms} = \sqrt{\langle \delta^2 \rangle} \propto M^{-(n+3)/6}$$

Similarly a power law spectrum implies a power-law correlation function. If

$$\xi(r) = \left(\frac{r}{r_0}\right)^{-\gamma}\,,$$

with $\gamma = n + 3$ we obtain

$$\Delta^2(k) = \frac{2}{\pi}(kr_0)^\gamma \Gamma(2-\gamma)\sin\frac{(2-\gamma)\pi}{2} \equiv \beta(kr_0)^\gamma\,,$$

which is only valid for $n < 0$. The general limit from asymptotic homogeneity requires $n > -3$. Furthermore, according to Zel'dovich, the discreteness

of matter requires $n < 4$. $n = 0$ is know as *white noise* because the power is the same on all scales.

A very important scale factor is $n = 1$, ie. $\Delta \propto k^4$. From Eqn. 4.9 we have

$$\delta\Phi_k \propto \frac{\delta_k}{k^2}$$

and hence from $\Delta^2 \propto k^3\delta_k^2$ we obtain

$$\Delta_\Phi^2 \propto \delta\Phi_k^2 k^3 = \text{const}$$

and hence for $n = 1$ the potential perturbations $\delta\Phi_k$ which govern the metric are *scale-invariant*.

A common way to normalize the power spectrum is normalize it to the observed fluctuations on an $8h^{-1}\,\text{Mpc}$ scale[2]. It is quite common to define the scale by a spherical *top-hat* window function with a real-space representation of

$$W(r) = \frac{V}{(4\pi)/3R_T^3}\,,$$

which is in Fourier space

$$\boxed{W(kR_T) = \frac{3}{(kR_T)^3}\left[\sin(kR_T) - (kR_T)\cos(kR_T)\right]\,. \quad (4.28)}$$

The normalization parameter is then

$$\boxed{\sigma_8^2 = 4\pi \int \frac{dk}{k} k^3 P(k) W^2(k8h^{-1}\,\text{Mpc})\,, \quad (4.29)}$$

which is the filtered variance on $8h^{-1}\,\text{Mpc}$. The measured σ_8 is currently between $0.75 - 1.1$ dependent on the measurement. There are two notes of caution required when comparing the normalization here with observations. First the measured powerspectrum is usually obtained from discrete, collapsed object where linear perturbation theory ($\delta \ll 1$) clearly breaks down. Furthermore one is usually observing (apart from lensing observations) the distribution of light, which does not necessarily have to follow the distribution of mass, particularly in the cold dark matter model. This might introduce a *bias* which is commonly parametrised with the bias parameter b.

[2]Remember that k in the power spectrum is the comoving wavenumber and this is why the factor h^{-1} appears in the scale.

4.2.1 Redshift Space Effects

So far we have discussed the power spectrum in 3-dimensional space. Usually one has information about the angular pattern and the redshift. However the redshift is modified by peculiar velocities (see Exercise !) with $1 + z \rightarrow (1 + z)(1 + \delta u/c)$. Since the peculiar velocities are related to the clustering ($\delta\rho$) the clustering in *redshift space* , if redshift is assumed to be from the Hubble expansion, differs systematically from realspace. In the large distance approximation we can assume that an objects subtends a small angle and the radial distortions are along a Cartesian axis. From Eqn. 4.11 we obtain

$$\delta\mathbf{u}_k = -\frac{iHf(\Omega)a}{k}\delta_k\hat{\mathbf{k}}\,,$$

with

$$f(\Omega) =\equiv \frac{a}{\delta}\frac{d\delta}{da}\,.$$

Note that $f\Omega)$ is called the velocity suppression factor, with $f(\Omega_{\rm m,0}) \approx \Omega_{\rm m,0}^{0.6}$. In real space the velocity perturbation and the displacement are related by

$$\delta\mathbf{u} = Hf(\Omega)\mathbf{x}\,.$$

In redshift space the apparent distance

$$\mathbf{r}_{\rm apparent} = \mathbf{r} + (\hat{\mathbf{r}}\cdot\mathbf{u}/H)\hat{\mathbf{r}} = \mathbf{r} + (\mu u/H)\mathbf{r}\,,$$

with $\mu = \hat{\mathbf{r}}\cdot\hat{\mathbf{k}}$. If we assume now a plane-wave disturbance running at some angle to the line of sight, producing a displacement field$\mathbf{x}$ parallel to $\mathbf{k}$, the apparent displacement is $\mathbf{x} + f(\Omega)\mu x\hat{\mathbf{r}}$. For determining the apparent amplitude along the wavevector we need $x + f(\Omega)\mu^2 x$. We then obtain

$$\delta_{\rm m,z} = \delta_{\rm m,r}\left[1 + f(\Omega)\mu^2\right]\,, \tag{4.30}$$

where $\delta_{\rm m,z}$ is the perturbation in real space and $\delta_{\rm m,r}$ in redshift space. If we assume that there is a linear constant bias between the distribution of light emitting mass $\delta_{\rm lem}$ and mass we obtain

$$\delta_{\rm lem} = b\delta_{\rm m} = \delta_{\rm m} + (b-1)\delta_{\rm m}\,.$$

The trivial rearrangement emphasises that the *observed* density fluctuation must be a combination of the dynamically generated density contrast plus the additional term due to bias, which might be different in different regions of space. Hence we realize that *the first term is associated with peculiar velocities, but the second is not.* We then obtain

$$\delta_{\rm lem,z} = \delta_{\rm m,r}\left[1 + f(\Omega)\mu^2\right] + (b-1)\delta_{\rm m,r} = \delta_{\rm lem,r}\left[1 + \frac{f(\Omega)\mu^2}{b}\right] . \quad (4.31)$$

When we define

$$\beta \equiv \Omega^{0.6}/b \quad (4.32)$$

we can write for the ratio of power spectra

$$\frac{P_z}{P_r} = \left(1 + \beta\mu^2\right)^2 .$$

Note that this approximation does not hold on small scales, where non-linear effects become important.

We can now finally discuss the power spectrum as measured from the 2dF galaxy redshift survey.

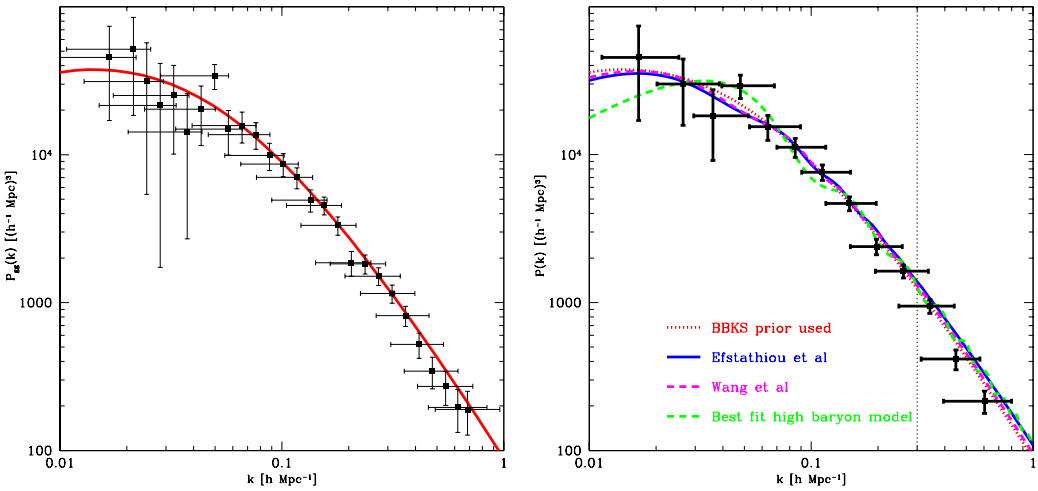

Figure 4.3: Galaxy-galaxy powerspectrum as measured from the 2dF survey (left) and binned data points with models [Tegmark et al. 2002]. Note that $\beta = 0.5$ is assumed.

4.3 Press-Schechter Formalism

We will now enter the are of non-linear perturbations and a descriptions and study a theory introduced by Press & Schechter 1974. Indeed in recent years it has been established that a full numerical simulation reveals only slight, although important, deviations from this scheme [Jenkins 2001].

> Press-Schechter theory assumes that if we smooth the linear density perturbations on some mass scale M, then the fraction of space in which the smoothed density field exceeds some critical threshold δ_c is in collapsed objects of mass greater than M.

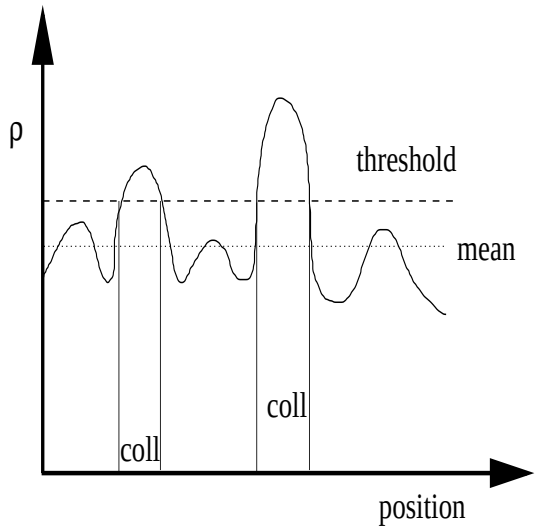

Figure 4.4: Schematic description of the Press-Schechter formalism.

We hence smooth the linear density field with the spherical top-hat in Eqn. 4.28. If we associate the mass of the cluster, before collapse, with the matter M and the background density $\rho_{\mathrm{m},0}$ we obtain for the radius R of this region

$$M = \frac{4\pi}{3}\rho_{\mathrm{m},0}R^3\,,$$

which we then can use to calculate the rms fluctuation $\sigma(M,z)$

$$\sigma^2(M,z) = 4\pi \int dk\, k^2 P(k) W^2(kR)\,.$$

In the next chapter we will find that the linear over-density required for collapse is $\delta_c \approx 1.69$. If we assume that the density field is a Gaussian we can then write for the probability that a given point in space has the over-density between δ and $\delta + d\delta$, smoothed on the mass scale M is $p_M(\delta)d\delta$, with

$$p_M(\delta) = \frac{1}{\sqrt{2\pi}\sigma} \exp\left\{-\frac{1}{2}\frac{\delta^2}{\sigma^2(M,z)}\right\} . \tag{4.33}$$

Then the probability of a point in space forming part of a cluster with radius larger than R is equal to the probability of the density field, after smoothing over scale M (R), having an over-density larger than the critical over-density δ_c. That is

$$\mathcal{P}_{>R} = \int_{\delta_c}^{\infty} p_M(\delta)\, d\delta\,.$$

To obtain the probability $\mathcal{P}_R\, dR$ of a point in space forming a cluster with radius between R and $R + dR$, we differentiate the above expression with respect to R and take the absolute value

$$\mathcal{P}_R\, dR = \left|\frac{d}{dR}\mathcal{P}_{>R}\right| dR\,.$$

We can then obtain the number density of such clusters by dividing through the cluster volume

$$n(R)dR = \frac{3f}{4\pi R^3}\left|\frac{d}{dR}\mathcal{P}_{>R}\right| dR\,, \tag{4.34}$$

where we have introduced a correction factor, whose value will ensure that the final mass function accounts for the entire mass in the universe. The number of clusters with mass larger than M is then

$$N_{>M} = \frac{3f}{4\pi}\int_R^{\infty}\frac{dR}{R^3}\left|\frac{d}{dR}\mathcal{P}_{>R}\right| .$$

To fix the value of the correction factor f we use for the mass density

$$\rho_{\mathrm{m},0} = \int_0^{\infty} M(R)n(R)\; dR$$

and we obtain with Eqns. 4.33 and 4.34 $f = 2$. If we include this factor into the probability density we obtain for the probability $\mathcal{P}_{>R}$

$$\mathcal{P}_{>R} = \mathcal{P}_{>M} = 1 - \mathrm{erf}\left[\frac{\delta_c}{\sqrt{2}\sigma(M,z)}\right] , \tag{4.35}$$

The power of the Press-Schechter model is that it leads to a mass function of collapsed (virialized; see next chapter) objects, ie. the number density of objects of a given mass. To obtain the comoving number density of objects of mass M, per mass interval dM, at redshift z, we perform, as above, the following: Differentiate Eqn. 4.35 with respect to the mass. If we multiply this by the comoving number density $\rho_{\rm m,0}$ we obtain the change in the mass density above the threshold. If we divide this by the mass M we obtain the comoving number density and we finally obtain, by applying the chain rule

$$\boxed{\frac{dn(M,z)}{dM}dM = -\sqrt{\frac{2}{\pi}}\frac{\rho_{\rm m,0}}{M}\frac{\delta_c}{\sigma^2(M,z)}\frac{d\sigma(M,z)}{dM}\exp\left(-\frac{\delta_c^2}{2\sigma^2(M,z)}\right)\,dM\,,} \tag{4.36}$$

which is the *Press-Schechter* mass function.

Figure 4.5: Left: structure in a N-body simulation. Right: the multiplicity function $f(\sigma) = Mdn(M,z)/d\ln\sigma^{-1}/\rho_{\rm m,0}$, with the dashed line for the Press-Schechter function from a simulation by the Virgo consortium [Jenkins, 2001].

Chapter 5

Clusters of Galaxies

In this final chapter we will move on to study the properties of truly non-linear structures on extra-galactic scales, namely clusters of galaxies. In order to obtain a theoretical description how these clusters might form we will study the behaviour of a spherical over-density in a flat matter dominated universe.

5.1 Spherical Collapse and Virialization

In Fig. 5.1 we show the set up for the spherical collapse model. The over-density δ of radius R is take from a thin shell with density zero in order to maintain the mean density. The universe inside the spherical over-density behaves according to Gauss law completely detached from the evolution of the surrounding universe, which itself is unaffected by the over-density because of the thin shell of zero density. The universe inside the over-density behaves like a closed universe with $\Omega_{\rm m} = 1 + \delta$. As we saw in Fig.2.3 such a universe will re-collapse in a finite time. From the analysis of a closed matter dominated universe in Sec. 2.1.5, Eqn. 2.24 we obtain

$$\begin{aligned} a &= (1 - \cos\theta)\frac{\Omega_{\rm m}}{2(\Omega_{\rm m} - 1)} \\ H_0 t &= (\theta - \sin\theta)\,\frac{\Omega_{\rm m}}{2(\Omega_{\rm m} - 1)^{3/2}}\,, \end{aligned} \tag{5.1}$$

where we have chosen the parametric solution. Expressing this in terms of the scale factor a_m and time t_m at maximum expansion from Eqn. 2.25 we obtain

$$\frac{a}{a_m} = \frac{1}{2}(1 - \cos\theta)\,, \qquad \frac{t}{t_m} = \frac{1}{\pi}\,(\theta - \sin\theta)\ .$$

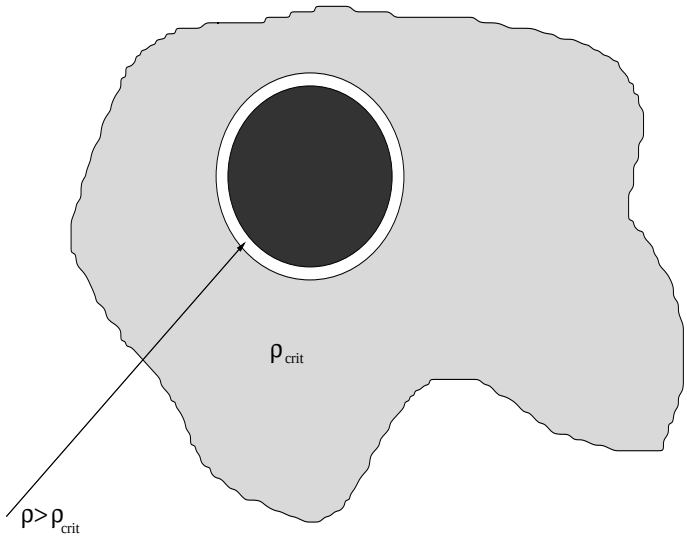

Figure 5.1: Spherical over-density, with "decoupled" evolution from the background universe.

To study the linear regime we need an expansion in θ and obtain

$$\frac{a}{a_m} \simeq \frac{\theta^2}{4} - \frac{\theta^4}{48}\,, \qquad \frac{t}{t_m} \simeq \frac{1}{\pi}\left(\frac{\theta^3}{6} - \frac{\theta^5}{120}\right)\,.$$

If we combine these we obtain the linearised scale factor with

$$\frac{a_{\rm lin}}{a_m} \simeq \frac{1}{4}\left(6\pi\frac{t}{t_m}\right)^{2/3}\left[1 - \frac{1}{20}\left(6\pi\frac{t}{t_m}\right)^{2/3}\right]\,. \tag{5.2}$$

Note that if we ignore the term in square brackets we just obtain the expansion of the background in a flat matter dominated universe. Including both terms gives the *linear theory* expression for the growth of a perturbation. Usually we call the point of maximum expansion *turnaround*, which is reached for $\theta = \pi$. Up to this point the general expansion of the universe has been dominating over the collapse and the physical size of the region was still growing. Because we are studying a matter dominated universe the energy densities are always $\propto a^{-3}$. Hence the relation between the linear over-density and the background density is

$$1 + \delta_{\rm lin} = \frac{a^3_{\rm back}}{a^3_{\rm lin}}\,,$$

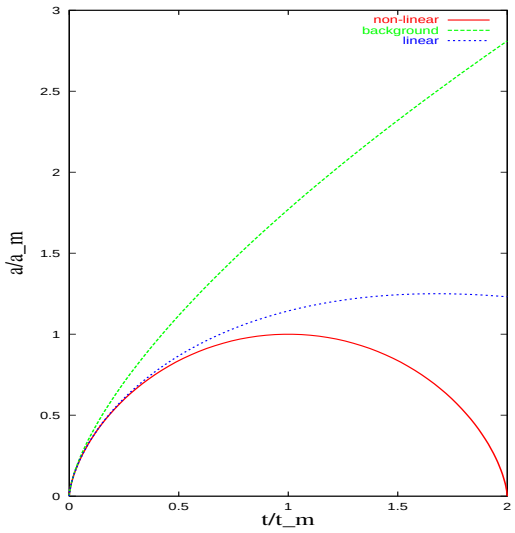

Figure 5.2: The evolution of the background scale factor, the linear scale factor and the non-linear, collapsing scale factor.

where $a_{\rm back}$ is given by the lowest order truncation of Eqn. 5.2. We then obtain (after linearising)

$$\delta_{\rm lin} = \frac{3}{20}\left(6\pi\frac{t}{t_{\rm m}}\right)^{2/3} .$$

So, at turnaround, $t = t_m$ we get

$$\delta_{\rm lin}^{\rm turn} = \frac{3}{20}(6\pi)^{2/3} = 1.06\,.$$

This tells us that at the breakdown of linear theory, where $\delta_{\rm lin}$ is unity, structures break away from the background evolution, but gravitationally bound structures have yet to form. After turnaround the collapse proceeds symmetrically to the expansion phase and the object collapses at $t = 2t_m$. At this time the linear density contrast has become

$$\delta_{\rm lin}^{\rm coll} = \delta_c = \frac{3}{20}(12\pi)^{2/3} = 1.686\,. \tag{5.3}$$

So the linear density contrast of about 1.7 corresponds to the epoch of complete gravitational collapse of a spherical symmetric perturbation. Note that this is exactly the critical over-density δ_c we used for the Press-Schechter model in the previous Section.

Ultimately we do not expect the object to collapse to a point but rather to reach virial equilibrium. This is reached when the radius has shrunk by a factor of 2 from that of turnaround. Numerical estimation show that $\delta_{\rm lin}^{\rm coll}$ is a good estimate for the epoch of virialization.

The actual nonlinear density contrast at turnaround is

$$1+\delta_{\rm nonlin}^{\rm turn}=\frac{a_{\rm back}^3}{a_{\rm max}^3}=\frac{(6\pi)^2}{4^3}=5.55\,.$$

In the spherical collapse model, the density goes infinite at the collapse time. However if we assume that the collapsing object virializes at half the radius[1]. Since the background scale factor is $\propto t^{2/3}$ the density of the background has fallen in the same time by a factor of 4. In combination the over-density at virialization is then $5.55\cdot 4\cdot 8$ and hence

$$\boxed{1+\delta_{\rm nonlin}^{\rm vir}\simeq 178} \qquad (5.4)$$

which is remarkably well verified by simulations. In a low density universe $\delta_{\rm lin}^{\rm coll}$ is hardly changed but the true density contrast at virialization is increased to $178\Omega_{\rm m,0}^{-0.6}$. Finally we obtain from the virial theorem for bound objects

$$v^2=\frac{GM}{R_g}\,,$$

where M is the mass of the system and R_g the radius where the gravitational energy is $-GM^2/R_g$. The mass within an initial comoving radius $R_{\rm com}$ is

$$M=\frac{4\pi}{3}\rho_{\rm m,0}R_{\rm com}^3\,.$$

The virial theorem tells us (see above) that the cluster collapses at half the turnaround radius, $R_g=R_{\rm turn}/2$. We then obtain

$$R_{\rm turn}^3=\frac{1}{5.55}R_{\rm phys}^3=\frac{1}{5.55}\frac{1}{(1+z_{\rm turn})^3}R_{\rm com}^3\,.$$

Because the virialization time is twice the time to the maximum and we assume matter domination, we have $1+z_{\rm turn}=2^{2/3}(1+z_{\rm vir})$ and hence with

$$R_g^3=\frac{1}{178}\frac{1}{(1+z_{\rm vir})^3}R_{\rm com}^3\,,$$

we obtain

[1]This can be obtained from the virial theorem $U_{\rm vir}=-2T_{\rm vir}$, with U the potential energy and T the kinetic energy. At turnaround the kinetic energy of the collapsing sphere is zero. With $U_{\rm turn}=U_{\rm vir}+T_{\rm vir}$ we obtain, since $U\propto 1/R$, $2R_{\rm vir}=R_{\rm turn}$.

$$\boxed{\left(\frac{v}{127\ \mathrm{km\ sec^{-1}}}\right)^2 = \left(\frac{M}{10^{12}h^{-1}M_\odot}\right)^{2/3}(1+z_{\mathrm{vir}})\ .} \quad (5.5)$$

The scaling of this relation is well established in numerical simulations however the normalization is different than in this rough analytical analysis. Note that objects with the same mass have a larger virial velocity because they are more compact because they formed when the Universe was smaller and denser. Galaxies have virial velocities of order 100 km sec^{-1}, whereas clusters have $1,000$ km sec^{-1}. If we assume that the cosmological fluid inside the cluster is in hydrostatic equilibrium, ie. the pressure is only provided by gravity, we can relate $T \propto v^2$ and hence obtain

$$\frac{k_{\mathrm{B}}T}{0.07\ \mathrm{keV}} = \left(\frac{M}{10^{12}h^{-1}M_\odot}\right)^{2/3}(1+z_{\mathrm{vir}})\ .$$

This gives rise to x-ray emissions of the hot gas.

5.2 X-ray Signatures

The main x-ray signature of a cluster is thought to be thermal bremsstrahlung of the diffuse hot intra-cluster gas.

5.2.1 Thermal Bremsstrahlung

Let's assume a region of size R containing charges with non-relativistic motion $v \ll c$. We will consider the radiation field at a distance L with $L \gg R$. The electro-magnetic field at $(t, \mathbf{r})$ depends on the behaviour of a charge at time t' with $ct' = ct - |\mathbf{r} - \mathbf{x}(t')|$ and $\mathbf{x}(t)$ the trajectory of the charge. For large distances we obtain

$$L \equiv |\mathbf{r} - \mathbf{x}(t')| \simeq r - \mathbf{x}\cdot\mathbf{n}\,,$$

where $\mathbf{n}$ is the unit vector $\mathbf{r}/r$. Also, in calculating the field at large distances, we can replace the L^{-1} in the Lienard-Wiechert potential (see for example Jackson, Electrodynamics Exercise !) with r^{-1} and ignore $\mathbf{v}\cdot\mathbf{n}/c$ in the denominator to obtain

$$\mathbf{A}(t,\mathbf{r}) = \frac{1}{cr}\sum_i q_i \mathbf{v}_i(t')\,, \qquad t' = t - \frac{r}{c} + \frac{\mathbf{x}\cdot\mathbf{n}}{c}$$

If T is the characteristic time in which the charge distribution changes, then the typical wavelength of emitted radiation is $\lambda \simeq cT$. With $(\mathbf{x}\cdot\mathbf{n})/c)$ is of the order of R/c. Hence we can ignore this term if $(R/c) \ll T$, or $R \ll \lambda$. This is satisfied if $v \ll c$ with v the typical velocity of the charges. Hence we can write

$$\mathbf{A}(t,\mathbf{r}) = \frac{1}{cr}\sum_i q_i \mathbf{v}_i[t-(r/c)] = \frac{\dot{\mathbf{d}}[t-(r/c)]}{cr}\,,$$

where $\mathbf{d} = \sum q_i \mathbf{x}_i$ is the dipole moment of the system and the sum is over all the charges in the system. This is a *dipole radiation field*.

The angular distribution of dipole radiation can be obtained as follows: At large distances from the system of charges, the electromagnetic wave may be treated as a plane wave. Then, noting that the vector potential depends on only $[t-(r/c)]$, we can write $\mathbf{B} = \nabla\times\mathbf{A} \simeq (\dot{\mathbf{A}}\times\mathbf{n})/c$ and $\mathbf{E} = \mathbf{B}\times\mathbf{n}$, we obtain for the dipole radiation

$$\mathbf{B} = \frac{1}{c^2 r}\left(\ddot{\mathbf{d}}\times\mathbf{n}\right)\,, \qquad \mathbf{E} = \frac{1}{c^2 r}\left(\ddot{\mathbf{d}}\times\mathbf{n}\right)\times\mathbf{n}\,.$$

The energy flux (Poynting vector) is given by $\mathbf{S} = c(\mathbf{E}\times\mathbf{B})/4\pi = c(B^2/4/pi)\mathbf{n}$ and hence the amount of energy propagating into a solid angle $d\Omega$ in unit time is $|\mathbf{S}|r^2 d\Omega$, giving

$$\frac{dE}{dtd\Omega} = |\mathbf{S}|r^2 = \frac{cB^2r^2}{4\pi} = \frac{1}{4\pi c^3}\left(\ddot{\mathbf{d}}\times\mathbf{n}\right)^2 = \frac{|\ddot{\mathbf{d}}|^2}{4\pi c^3}\sin^2\theta\,, \qquad (5.6)$$

where the right hand side should be evaluated at the retarded time.

The spectral composition of radiation, e.g. the amount of energy that is radiated by the system between frequencies ω and $\omega + d\omega$, can be obtained as follows: The Fourier transform of $\mathbf{B}(t)$ is $\mathbf{B}(\omega) = (c^2 r)^{-1}[\ddot{\mathbf{d}}(\omega)\times\mathbf{n}$, with $\ddot{\mathbf{d}}(\omega) = -\omega^2\mathbf{d}(\omega)$. With

$$\int_{-\infty}^{+\infty} B^2(t)dt = \int_{-\infty}^{+\infty}|\mathbf{B}(\omega)|^2\frac{d\omega}{2\pi} = 2\int_0^{\infty}|\mathbf{B}(\omega)|^2\frac{d\omega}{2\pi}$$

and we can write Eqn. 5.6

$$\frac{dE}{d\Omega} = \frac{cr^2}{4\pi}\int_{-\infty}^{+\infty}B^2(t)dt = \frac{cr^2}{2\pi}\int_0^{\infty}|\mathbf{B}(\omega)|^2\frac{d\omega}{dt}\,,$$

which results in

$$\frac{dE}{d\omega d\Omega} = \frac{cr^2|\mathbf{B}(\omega)|^2}{4\pi^2} = \frac{\omega^4|\mathbf{d}(\omega)|^2}{4\pi^2 c^3}\sin^2\theta\,. \qquad (5.7)$$

This expression give the amount of energy radiated into a solid angle $d\Omega$ and frequency range $d\omega$.

Consider now the situation in which the velocity of a charged particle changes from $\mathbf{v}_1$ to $\mathbf{v}_2$ in a short time τ. In this case very little radiation will be emitted at frequencies higher than $\omega_0 \approx 1/\tau$ and we obtain

$$\mathbf{B}(\omega) \equiv \int_{-\infty}^{+\infty} \mathbf{B}(t) e^{-i\omega t} dt \simeq \int_{-\infty}^{+\infty} \mathbf{B}(t) dt$$

for $\omega \ll \tau^{-1}$. With $\mathbf{B} = (\dot{\mathbf{A}} \times \mathbf{n})/c$ we obtain

$$c\mathbf{B}(\omega) = -\mathbf{n} \times \int_{-\infty}^{+\infty} \dot{\mathbf{A}} dt = -\mathbf{n} \times [\mathbf{A}_2 - \mathbf{A}_1] \,,$$

where $\mathbf{A}_1$ and $\mathbf{A}_2$ are the initial and final values of the vector potential. Then we obtain with Eqn. 5.7

$$\frac{dE}{d\omega d\Omega} = \frac{cr^2 |\mathbf{B}(\omega)|^2}{4\pi^2} = \frac{r^2}{4\pi^2 c} \left[(\mathbf{A}_2 - \mathbf{A}_1) \times \mathbf{n} \right]^2 \,.$$

We obtain the vector potential from the Lienard-Wiechert formula

$$\mathbf{A} = \frac{q\mathbf{v}}{cr[1 - (\mathbf{v} \cdot \mathbf{n})/c]} \simeq \frac{q\mathbf{v}}{cr} \,,$$

where we applied the non-relativistic approximation. We then obtain

$$\frac{dE}{d\omega d\Omega} \simeq \frac{q^2}{4\pi^2 c^3} \left[(\mathbf{v}_2 - \mathbf{v}_1) \times \mathbf{n} \right]^2 = \frac{q^2}{4\pi^2 c^3} (\Delta v)^2 \sin^2 \theta \,.$$

The total energy emitted over all directions is then obtained by integrating over $d\Omega$ and we finally get

$$\frac{dE}{d\omega} = \frac{2}{3\pi} \frac{q^2}{c^3} (\Delta v)^2 \,. \tag{5.8}$$

Note that the energy emitted per unit frequency interval is independent of ω for $\omega \ll \tau^{-1}$, while there is very little energy emitted for $\omega \gg \tau^{-1}$.

In a plasma the electrons are constantly accelerated during their collision with ions, which leads to the emission of radiation by the plasma called thermal bremsstrahlung.

We consider now an individual scatter event between an electron and an ion of charge Ze. The electron has an initial velocity v and the impact

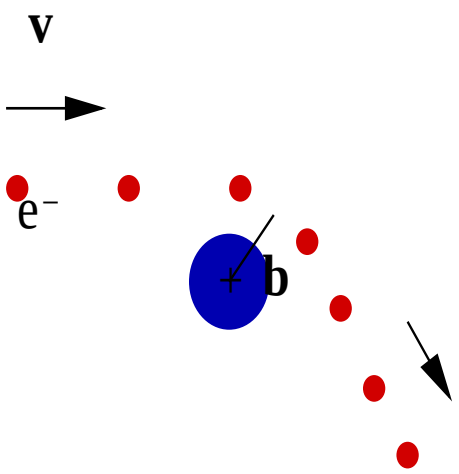

Figure 5.3: Scattering of an electron at an ion, with impact parameter b.

parameter (point of closest approach of the electron to the ion) is b. The Coulomb force leads then to an acceleration of the electron of

$$a \simeq \frac{Ze^2}{m_e b^2}\,,$$

which lasts a typical time $t = 2b/v$. Hence we obtain a velocity change

$$\Delta v = at = \frac{Ze^2}{m_e b^2}\frac{2b}{v}\,.$$

Because the scattering lasts for a time $t = 2b/v$ there will be very little power at frequencies $\omega > \omega_{\rm max} \simeq v/2b$. From Eqn. 5.8 we then obtain

$$\frac{dE}{d\omega} = \frac{2}{3\pi}\frac{e^2}{c^3}\left(\frac{Ze^2}{m_e b^2}\frac{2b}{v}\right)^2 = \frac{8}{3\pi}\frac{Z^2e^6}{m_e^2c^3}\left(\frac{1}{vb}\right)^2\,. \tag{5.9}$$

This is the amount of radiation emitted in a single collision. If the number density of ions n_i and electrons n_e are the same $n_i = n_e = n$, then the total amount of energy emitted per unit volume per second that is due to all collisions with impact parameter in the range $(b, b+db)$ will be

$$\left(\frac{dE}{dV\,d\omega dt}\right)_{\rm total} = n_i n_e v(2\pi b\;db\;)\frac{dE}{d\omega} = n^2 v\;db\;\left(\frac{dE}{d\omega}\right)2\pi b = \frac{16Z^2e^6n^2}{3m_e^2c^3v}\frac{1}{b}\;db\,.$$

Integrating over b in the limits b_1 and b_2 we obtain

$$\left(\frac{dE}{dV\,d\omega dt}\right) = \frac{16Z^2e^6n^2}{3m_e^2c^3v}\ln\left(\frac{b_2}{b_1}\right) = \frac{16\pi Z^2e^6n^2}{3\sqrt{3}m_e^2c^3}\frac{1}{v}g_{ff}(v,\omega)\,, \tag{5.10}$$

where we have introduced the Gaunt factor

$$g_{ff}(v,\omega) = \frac{\sqrt{3}}{\pi} \ln\left(\frac{b_2}{b_1}\right) .$$

The upper limit b_2 is determined by the fact that most of the radiation comes from $\omega < v/2b$ and therefore $b < v/\omega$. Note that the lower limit is determined by the kinetic energy of the electron and quantum effects. g_{ff} is altogether a *slowly* varying function of velocity and frequency.

We can now move on to average the emission over the velocity distribution of the electrons. For a plasma in thermal equilibrium the electrons have a Maxwell distribution of velocities. Since an electron needs to have a minimum energy $\frac{1}{2}m_e v_{\rm min}^2 \simeq \hbar\omega$ to emit a photon of energy $\hbar\omega$, the averaging of $1/v$ will lead to a factor

$$\begin{aligned} \left\langle \frac{1}{v} \right\rangle &= \left(\frac{m_e}{2\pi k_B T}\right)^{3/2} \int_{v_{\rm min}}^{\infty} \frac{1}{v} 4\pi v^2 \, dv \, \exp\left[-\frac{m_e v^2}{2k_B T}\right] \\ &= \sqrt{\frac{2m_e}{\pi k_B T}} \exp\left(-\frac{\hbar\omega}{k_B T}\right) . \end{aligned} \tag{5.11}$$

We finally obtain as the *specific emissivity*

$$j(\omega) = \frac{dE}{dV dt d\omega} = \frac{16\pi Z^2 e^6 n^2}{3\sqrt{3} m_e^2 c^3} \left(\frac{2m_e}{\pi k_B T}\right)^{1/2} \exp\left(-\frac{\hbar\omega}{k_B T}\right) \bar{g}_{ff}(\omega) \propto n^2 T^{-1/2} , \tag{5.12}$$

with $\bar{g}_{ff}(\omega)$ the velocity averaged Gaunt factor which can vary between 1 and 5. As discussed in the previous section about spherical infall, it is thought that the intra-cluster gas is heated during its formation process.

5.2.2 X-ray Observables

Including numerical Gauntfactors a good approximation for the net free-free luminosity is

$$J = \int d\omega j(\omega) \approx 1.42 \times 10^{-27} T^{1/2} n^2 \text{ erg cm}^{-3} \text{ sec}^{-1} ,$$

where we have introduced the energy unit erg which is typically used in x-ray astronomy and is erg $= 10^{-7}$ Joule. If we assume that the temperature

across the cluster is uniform (isothermal) and has an electron density

$$n(r) = \frac{n_c}{1 + r^2/r_c^2} \tag{5.13}$$

we can calculate the total bremsstrahlung luminosity L_X of the cluster with

$$L_X = \int J \, d^3r = 1.4 \times 10^{42} n_c(\mathrm{cm}^{-3})^2 r_c(\mathrm{kpc})^3 T_X(\mathrm{keV})^{1/2} \text{ erg sec}^{-1} ,$$

where n_c is the central electron number density n_c measured in units of cm^{-3} and the core radius r_c in kiloparsecs. A typical value for the cluster x-ray luminosity is

$$L_X \sim 1 \times 10^{44} h^{-2} \text{ erg sec}^{-1} .$$

For the core radius, density and temperature of the plasma typical values are

$$r_c \sim 200 h^{-1} \text{ kpc} , \qquad T_X \sim 4 \text{ keV} , \qquad n_c \sim 0.003 h^{1/2} \text{ electrons/cm}^3 .$$

Figure 5.4: On the left the Hydra cluster from an optical observation on La Palma (B. MacNamara) and on the right the same region observed with the Chandra X-ray satellite.

Hydra A in Fig. 5.4 is a galaxy cluster that is 840 million light years from Earth (redshift $z = 0.054$). Optical observations show a few hundred galaxies in the cluster. Chandra X-ray observations reveal a large cloud of

hot gas that extends throughout the cluster. The gas cloud is several million light years across and has a temperature of about 40 million degrees in the outer parts decreasing to about 35 million degrees in the inner region.

In general the observed X-ray spectra are generally fit fairly well by Eqn. 5.12 with gas temperatures of 2×10^7 to 10^8 K. The equation predicts the observed rapid fall off of the spectrum at high frequencies. If we relate the temperature of the gas to the mean kinetic energy of the atoms in the gas we find

$$\frac{k_B T}{\mu m_p} \approx \sigma_r^2 \,,$$

where μ is the mean atomic weight and m_p is the proton mass. This inferred velocity is similar to typical line of sight velocities σ_r of galaxies in the cluster. This is because the gas is exposed to the *same* gravitational potential as the galaxies.

5.3 Sunyaev-Zel'dovich Effect

Another signature we obtain from clusters of galaxies is the imprint of the Compton scattering of the CMB photons off the hot electrons of the intracluster medium, i.e.

$$\mathrm{e}^- + \gamma \rightarrow \mathrm{e}^{-\prime} + \gamma' \,.$$

The spectrum of the CMB radiation is to very high accuracy Planckian as can be seen in Fig. 5.5. Since Compton scattering conserves the number of photons, their energy gain is obtained by redistribution in frequency and hence distortion of the Planckian spectrum.

5.3.1 Kompaneets Equation

We will first discuss how a homogenous, isotropic distribution of photons is elastically scattered by a homogenous non-relativisitc gas of hot electrons. The net effect of many scatterings by the moving electrons produces a random walk in the energy of each photon, while conserving the photon number. As usual in scattering calculation we move between the laboratory frame (no subscripts), to the initial restframe of the electron before the scattering (subscript 1) to the primed quantities after scattering.

If the electron moves along the x-axis with velocity v in the laboratory frame we obtain with Lorentz transformation

$$t = \gamma(t_1 + v x_1) \,, \qquad x = \gamma(x_1 + v t_1) \,.$$

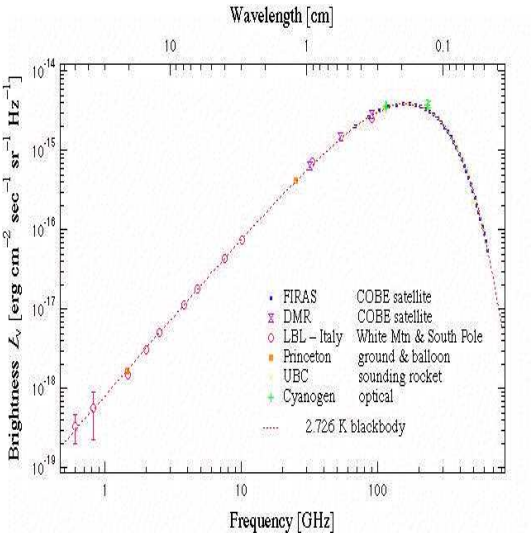

Figure 5.5: The CMB spectrum as measured by COBE (including errorbars !).

The same transformation can be applied to the energy and momentum of a photon of frequency ν which moves along an angle θ to the electron

$$\nu = \gamma\nu_1(1 + v\cos\theta_1)\,, \qquad \nu\cos\theta = \gamma\nu_1(\cos\theta_1 + v)\,.$$

The ratio of these two equations results in

$$\cos\theta = \frac{\cos\theta_1 + v}{1 + v\cos\theta_1}\,,$$

which is the transformation of the angle θ. The derivative of this expression gives the transformation of the solid angle $d\Omega = d(\cos\theta)d\phi$ of a beam of photons,

$$d\Omega = \frac{d\Omega_1}{\gamma^2(1 + v\cos\theta_1)^2}\,,$$

where we have used $\gamma^{-2} = 1 - v^2$.

Because of Liouville's theorem (constant phase space) the photon occupation number $\mathcal{N}$ is a Lorentz scalar quantity in the absence of collisions and hence

$$\mathcal{N}_1(\theta_1, \nu_1, t_1, x_1) = \mathcal{N}(\nu = \gamma\nu_1(1 + v\cos\theta_1), t = \gamma(t_1 + vx_1))\,. \qquad (5.14)$$

Finally we can write for the Boltzmann collision equation the the electron rest frame,

$$\frac{\partial \mathcal{N}_1}{\partial t_1} + \cos\theta_1 \frac{\partial \mathcal{N}_1}{\partial x_1} = R_1 \,,$$

where the right hand side is the rate R_1 of scattering of photons into the beam, less the rate of scattering out of the beam as seen by an observer in the electron rest frame. The left hand side is the derivative moving with the photon beam. From Eqn. 5.14 we obtain further

$$\frac{\partial \mathcal{N}_1}{\partial t_1} = \gamma \frac{\partial \mathcal{N}}{\partial t} \,, \qquad \frac{\partial \mathcal{N}_1}{\partial x_1} = \gamma v \frac{\partial \mathcal{N}}{\partial t}$$

and we obtain as the collision equation

$$\gamma \frac{\partial \mathcal{N}}{\partial t} \left(1 + v\cos\theta_1\right) = R_1 \,.$$

If we use the inverse energy transformation $\nu_1 = \gamma\nu(1 - v\cos\theta)$ we obtain

$$\gamma(1 - v\cos\theta) = \frac{1}{\gamma(1 + v\cos\theta_1)}$$

and hence

$$\frac{\partial \mathcal{N}}{\partial t} = \langle \gamma(1 - v\cos\theta) R_1 \rangle_\theta \,. \tag{5.15}$$

The brackets indicate averaging over the photon direction to get the time evolution of the occupation number in the laboratory frame.

Now we have to adress the scattering rate, R_1, where we have to take account of the electron recoil because the order of our calculation is $\mathcal{O}(v^2)$. In the initial electron rest frame the electron momentum is zero before scattering and afterwards

$$m_e \mathbf{v}_1' = \nu_1 \hat{\mathbf{k}}_1 - \nu_1' \hat{\mathbf{k}}_1' \,.$$

The square of this expression gives the final kinetic energy of the electron, which is the energy lost by the photon. To lowest non-trivial order this is the Compton shift

$$\nu_1 - \nu_1' = \delta\nu_1 = \frac{\nu_1^2}{m_e}(1 - \cos\Theta) \,,$$

with Θ the scattering angle. The rate of change of the number of photons in a beam of solid angle $d\Omega_1$ and bandwidth ν_1 to $\nu_1 + d\nu_1$, measured in the initial rest frame of the electron is then

$$R_1 \nu_1^2 d\nu_1 d\Omega_1 = \frac{d}{dt_1} \mathcal{N}_1(\theta_1, \nu_1) \nu_1^2 d\nu_1 d\Omega_1 = \int \frac{d\sigma}{d\Omega_s} I \,,$$

where on the right hand side the differential scattering cross section is integrated over the intensity I with

$$\begin{aligned} I &= [1+\mathcal{N}_1(\theta_1,\nu_1)]\left[\mathcal{N}_1(\theta_1',\nu_1^+)(\nu_1^+)^2 d\nu_1^+ d\Omega_1'\right] d\Omega_1 \\ &\quad -\left[1+\mathcal{N}_1(\theta_1',\nu_1^-)\right]\left[\mathcal{N}_1(\theta_1,\nu_1)\nu_1^2 d\nu_1 d\Omega_1\right] d\Omega_1' \,, \end{aligned} \tag{5.16}$$

with

$$\begin{aligned} \nu_1^\pm &= \nu_1 \pm \delta\nu \\ &= \nu_1\left[1 \pm \frac{\nu_1}{m_e}(1-\cos\Theta)\right] . \end{aligned} \tag{5.17}$$

The second line in Eqn. 5.16 gives the rate of scattering out of the beam. The second factor in this line in square brackets is the number of photons in the beam element. In the stimulated emission factor in front of it, the ocupation number is evaluated at the direction and frequency of the emitted photon. The frequency of the emitted photon is lowered by the Compton effect to ν_1^-. These photons are scattered into the solid angle $d\Omega_1'$, with cross section $d\sigma/d\Omega_s$ at a scattering angle Θ. The first line in Eqn. 5.16 is the rate of scattering into the beam element. Here the Compton effect requires that the incident photon has the energy $\nu_1^+ = \nu_1 + \delta\nu$. Here the incident beam with solid angle $d\Omega_1'$ is scattered into the beam with solid angle $d\Omega_1$. Note that we are ignoring the energy dependence of the cross section, because we are performing our analysis in the non-relativistic limit to order ν_1/m_e.

The next step is to write the occupation numbers in Eqn. 5.16 in the laboratory frame, with

$$\nu^\pm = \nu_1^\pm\gamma\left(1+v\cos\theta_1'\right) = \nu\frac{\nu_1^\pm}{\nu_1}\frac{1+c\cos\theta_1'}{1+v\cos\theta_1} .$$

We can now expand this expression to order $\mathcal{O}(v^2)$ and $\mathcal{O}(\nu/m_e)$ and obtain

$$\begin{aligned} \nu^\pm &= \nu\left[1\pm(\nu/m_e)(1-\cos\Theta)+v(\cos\theta_1'-\cos\theta_1)+v^2(\cos^2\theta_1-\cos\theta_1'\cos\theta_1)\right] \\ &\equiv \nu\pm\Delta^\pm \end{aligned} \tag{5.18}$$

and we obtain

$$\mathcal{N}_1(\theta_1,\nu_1) = \mathcal{N}(\nu) , \qquad \mathcal{N}_1(\theta_1',\nu_1^\pm) - \mathcal{N}(\nu\pm\Delta^\pm) .$$

We can now use Eqn. 5.16 to work out the rate R_1 and include this into Eqn. 5.15. The only additional ingredient we require is the momentum volume element

$$(\nu_1^+)^2 d\nu_1^+ = \left[1+4\frac{\nu_1}{m}(1-\cos\Theta)\right]\nu_1^2 d\nu_1 .$$

We then obtain

$$\frac{\partial \mathcal{N}}{\partial t} = \int \gamma(1 - v\cos\theta)\frac{d\Omega}{4\pi}\frac{d\sigma}{d\Omega_s}d\Omega_1'(A + B)\,, \tag{5.19}$$

with

$$A = \frac{4\nu}{m_e}(1 - \cos\Theta)\mathcal{N}(\nu)[1 + \mathcal{N}(\nu)]$$

and

$$B = [1 + \mathcal{N}(\nu)]\mathcal{N}(\nu + \Delta^+) - [1 + \mathcal{N}(\nu + \Delta^-)]\mathcal{N}(\nu)\,.$$

The integration over $d\Omega/4\pi$ corresponds to the averaging in Eqn. 5.15. We can now expand B to second order in electron speed v and obtain

$$\begin{aligned} B &= (1 + \mathcal{N})\left[\mathcal{N} + \frac{d\mathcal{N}}{d\nu}\Delta^+ + \frac{1}{2}\frac{d^2\mathcal{N}}{d\nu^2}(\Delta^+)^2\right] \\ &\quad -\mathcal{N}\left[1 + \mathcal{N} + \frac{d\mathcal{N}}{d\nu}\Delta^- + \frac{1}{2}\frac{d^2\mathcal{N}}{d\nu^2}(\Delta^-)^2\right]\,. \end{aligned}$$

If we calculate $A + B$ including the expressions for $\Delta^\pm$ we realize $A + B$ is of 1st order in v. Hence we only require 1st order terms in all subsequent approximations. We can then re-express the integration over the solid angle in Eqn. 5.19 to the relevant order

$$(1 - v\cos\theta)d\Omega = (1 - 3v\cos\theta_1)d\Omega_1\,.$$

Since $A + B$ is of order v we can use the classical Thomson scattering cross section ($\sigma_T = 6.65 \times 10^{-25}$ cm^2) which is symmetric under $\theta_1 \to \theta_1 + \pi$ and $\theta_1' \to \theta_1' + \pi$, so all odd terms in $\cos\theta_1$ and $\cos\theta_1'$ vanish in the integral. If we perform the final integration we than obtain

$$\frac{\partial \mathcal{N}}{\partial t} = \int \frac{d\Omega_1 d\Omega_1'}{4\pi}\frac{d\sigma}{d\Omega_s}(1 - 3v\cos\theta_1)(A + B) = \sigma_T C\,,$$

with

$$C = \frac{\nu}{m_e}\left[4\mathcal{N}(1 + \mathcal{N}) + (1 + 2\mathcal{N})\nu\frac{d\mathcal{N}}{d\nu}\right] + \frac{4}{3}\frac{d\mathcal{N}}{d\nu}\nu v^2 + \frac{1}{3}\frac{d^2\mathcal{N}}{d\nu^2}\nu^2 v^2\,.$$

This is the expectation value for scattering by a single electron. For a gas of electrons with number density n_e and mean square velocity $< v^2 >$ we obtain the Kompaneets equation

$$\frac{1}{\sigma_T n_e}\frac{\partial \mathcal{N}}{\partial t} = \frac{\nu}{m_e}\left[4\mathcal{N}(1+\mathcal{N}) + (1+2\mathcal{N})\nu\frac{\partial \mathcal{N}}{\partial \nu}\right] + \frac{4}{3}\left\langle v^2\right\rangle \nu\frac{\partial \mathcal{N}}{\partial d\nu} + \frac{1}{3}\left\langle v^2\right\rangle \nu^2\frac{\partial^2 \mathcal{N}}{\partial \nu^2}\,. \tag{5.20}$$

5.3.2 Sunyaev Zel'dovich effect

We can now move on to discuss the effect of hot intracluster gas in a rich cluster of galaxies on the CMB photons. The plasma is much hotter than

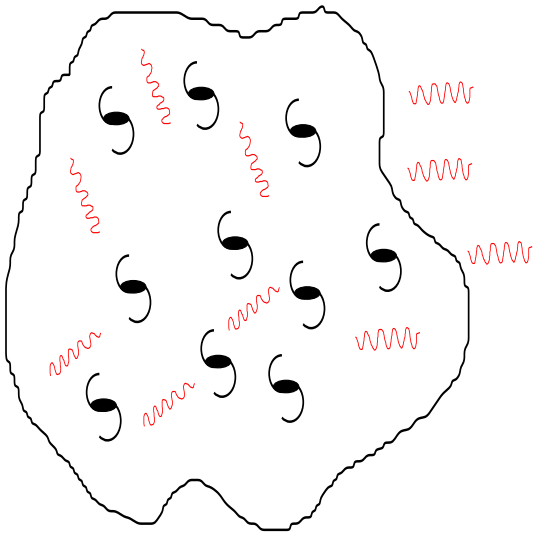

Figure 5.6: Scattering of CMB photons by hot intracluster gas.

the CMB and hence the terms with the kinetic factor $< v^2 >$ are dominating the Kompaneets equation Eqn. 5.20. In this case we have

$$\frac{1}{\sigma_T n_e c}\frac{\partial \mathcal{N}}{\partial t} = \frac{\left\langle v^2\right\rangle}{3c^2}\left[\nu^2\frac{\partial^2 \mathcal{N}}{\partial \nu^2} + 4\nu\frac{\partial \mathcal{N}}{\partial \nu}\right]\,. \tag{5.21}$$

If the electrons have a Maxwell-Boltzmann energy distribution at temperature T_e we have

$$\left\langle v^2\right\rangle = \frac{3k_B T_e}{m_e}\,.$$

We can rewrite Eqn. 5.21 more compact if we introduce

$$x = \frac{h\nu}{k_B T_e}\,, \qquad dy = \frac{k_B T_e}{m_e c^2}\sigma_T n_e c\; dt = \frac{\left\langle v^2 \right\rangle}{3c^2}\sigma_T n_e c\; dt$$

and obtain

$$\frac{\partial \mathcal{N}}{\partial y} = x^2 \frac{\partial^2 \mathcal{N}}{\partial x^2} + 4x \frac{\partial \mathcal{N}}{\partial x}\,.$$

As mentioned before the CMB is a nearly perfect black body with

$$\mathcal{N} = \frac{1}{e^{h\nu/k_B T_\gamma} - 1}\,.$$

We if we assume that the perurbations to the Planckian distribution are small we can write as the solution $\mathcal{N} + \delta\mathcal{N}$ and hence

$$\frac{\partial \mathcal{N}}{dy} = \frac{\delta \mathcal{N}}{y} \tag{5.22}$$

with

$$\boxed{y = \frac{k_B T_e}{m_e c^2}\int^t \sigma_T n_e c\; dt\,, \qquad (5.23)}$$

which is proportional to the pressure in the electron gas $n_e k_B T_e$. This can also be interpreted as the product between the gas temperature measured in units of electron mass and the scattering optical depth $\tau = \int \sigma_T n_e c\; dt$. We then obtain for Eqn. 5.22

$$\begin{aligned} \frac{\delta \mathcal{N}}{\mathcal{N}} &= y\left[\frac{x^2 e^x (e^x+1)}{(e^x-1)^2} - \frac{4x e^x}{e^x - 1}\right] \\ &\rightarrow \begin{cases} -2y & \text{at } x \ll 1\,, \\ \\ x^2 y & \text{at } x \gg 1\,. \end{cases} \end{aligned} \tag{5.24}$$

Hence the perturbed spectrum in the long wavelength limit, $x \ll 1$, where $\mathcal{N} \propto T_\gamma$, has the thermal Rayleigh-Jeans form with the effective temperature lowered by

$$\frac{\delta T_\gamma}{T_\gamma} = -2y\,. \tag{5.25}$$

Sunyaev and Zel'dovich (1972) pointed out that the plasma in a rich cluster is hot enough to upscatter the photons, increasing the surface brightness at

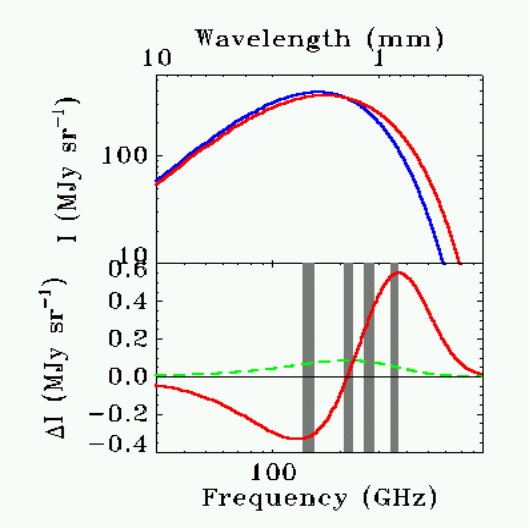

Figure 5.7: Spectral distortion due to SZ effect (S. Church). Lower panel, differential effects (green is the kinematic SZ effect due to the peculiar motion of the cluster). The bands are the frequency bands of the SuZie instrument.

short wavelength, and lowering the effective temperature at long wavelength.

If we assume an isothermal profile (Eqn. 5.13) with a constant temperature T_X we obtain for the optical depth at a distance R from the cluster centre

$$\tau = \sigma_T \int n(r) dl = \frac{\tau_0}{(1 + R^2/r_c^2)^{1/2}} ,$$

with

$$\tau_0 = 0.0064 n_c(\mathrm{cm}^{-3}) r_c(\mathrm{kpc}) ,$$

with $r_c \sim 200 h^{-1}$ kpc and $n_c \sim 0.003 h^{1/2}$ electrons/cm^3 we obtain

$$\tau_0 \sim 0.003 h^{-1/2} .$$

For the long wavelength side of the CMB spectrum the temperature as seen through the centre of the cluster is lowered by

$$\frac{\delta T_\gamma}{T_\gamma} = -2\tau_0 \frac{k_B T_X}{m_e c^2} \sim -5 \times 10^{-5} h^{-1/2}$$

This temperature decrement should be roughly constant over the core of the cluster, which extends an angle

$$\theta = \frac{2r_c}{d_A(z)} \approx \frac{2H_0 r_c}{cz} \sim \frac{0.5}{z} \text{ arcmin}\,,$$

where the approximation is for low redshifts $z \ll 1$.

We can now look at some Sunyaev Zel'dovich observations, of which some have been pioneered by the Astrophysics group at the Cavendish laboratory.

Figure 5.8: The Ryle telescopes at Lord's bridge Cambridge.

The Ryle telescope array consists of 8 individual parabolic 13m antennas observing at 15 GHz (2cm). It is common to talk in terms of a flux decrement instead of a temperature decrement which is given by

$$S_\nu = 2\nu^2 \Delta T f(x)\,,$$

with $f(x) = x^2 e^x [x/\tanh(x/2) - 4]/(e^x - 1)^2$. Usually the flux in radio astronomy is given in units of Jansky with $1\text{Jy} = 10^{-26}\text{J}/(\text{sec m}^2\text{ Hz})$.

Finally we should note that the SZ effect is an excellent probe for clusters at large redshifts because the dimming of the flux due to redshift is exactly canceld by the increased CMB photon energy density at larger redshifts.

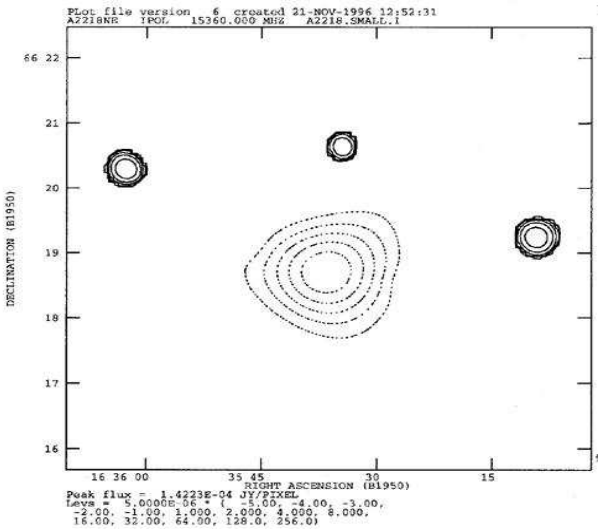

Figure 5.9: The cluster A2218 as observed with the Ryle telescope. The central flux decrement is 500 ± 70 μJy, corresponding to a temperature decrement of 0.09 mK (Jones & Grainge 1993).

Figure 5.10: Another observation of Abell 2218, with the BIMA array at 28.5 GHz. The contours are lines of constant flux decrement. The colours are intensities from X-ray emission of the hot gas as observed by the ROSAT satellite (Carlstrom et al.).